NOAA Technical Report ERL 380-WPL 49

Infrasound from Convective Storms, Part II: A Critique of Source Candidates

T.M. Georges

October 1976

U.S. DEPARTMENT OF COMMERCE
National Oceanic and Atmospheric Administration
Environmental Research Laboratories

NOAA Technical Report ERL 380-WPL 49

Infrasound from Convective Storms, Part II: A Critique of Source Candidates

T.M. Georges

Wave Propagation Laboratory
Boulder, Colorado

October 1976

U. S. DEPARTMENT OF COMMERCE
Elliot Richardson, Secretary

National Oceanic and Atmospheric Administration
Robert M. White, Administrator

Environmental Research Laboratories
Wilmot Hess, Director

CONTENTS

ABSTRACT

I critically examine several acoustic radiation mechanisms that have been suggested to explain the ultra-low-frequency emissions from certain severe thunderstorms that are observed on the ground and in the ionosphere. The candidates are: (a) simple acoustic sources (monopole, dipole) related to the expansion of heated storm air and to the storm-scale circulation pattern; (b) the random acoustic noise from "turbulent" motions inside storms; (c) low-frequency thunder, i.e., the radiation from lightning discharges or electrostatic relaxation inside storms; (d) vortex sound, the radiation from several kinds of unsteady vorticity or the interaction of multiple-vortex systems; and (e) thermo-mechanical oscillations driven by the interaction between latent-heat release and the storm's updraft. Each mechanism is evaluated for realism in terms of actual storm processes, and the predicted acoustic power and its spectral content are compared with those required by acoustic measurements. The mechanism most consistent with the observations appears to be a form of vortex radiation, in which instabilities and, ultimately, multiple vortices form about the periphery of a larger, mesoscale vortex, and radiate narrow-band sound as they spin about a common axis.

INFRASOUND FROM CONVECTIVE STORMS, PART II: A CRITIQUE OF SOURCE CANDIDATES

T. M. Georges

1. RATIONALE

One of the most persistent problems arising from observations of acoustic-gravity waves in the atmosphere has been identifying natural sources of the waves and establishing their radiation mechanisms. In many cases, empirical associations have been found between certain kinds of waves and particular geophysical phenomena, but even so, the number of completely satisfactory models of source mechanisms is small indeed. Emission processes are so elusive mainly because the kinds of direct atmospheric observations we would like are not available in sufficient quantity or with sufficient resolution; consequently, we are usually forced to adopt rather indirect and inductive approaches in searching for the correct mechanisms.

This report is about my search for a satisfactory model of the infrasound that some severe convective storms radiate. I have given necessary background information in Part I (Georges, 1973), which summarized what was then known about two different manifestations of the waves: one in radio soundings of the ionospheric F region, the other in recordings of microbarometric pressure fluctuations at the earth's surface. For brevity, that background will not be repeated here.

In discussing the plausibility of various possible mechanisms with colleagues, I have been consistently met with responses like, "Yes, but have you considered such-and-such mechanism?", usually with the implication that "their" mechanism is the obvious one to consider. These encounters led me to present my analysis of the source mechanism as a juxtaposition of the many that have been suggested. It is not my purpose to set up straw men to be sacrificed to a mechanism that I have known all along to be the correct one; when I began this analysis, each candidate appeared to have merits that could not be dismissed easily, and each of them required quantitative testing. The objective of this testing was to identify the "most likely" of the proposed models, based on a comparison with known wave observables and some simple theoretical arguments.

The analysis of the several source mechanisms spans diverse physical disciplines. This, in addition to the requirement for a thorough understanding of severe-storm dynamics, suggested that this should be a review paper containing more than the customary amount of tutorial material. At the expense of some redundancy, I have arranged the contents so that some sections can be skipped or passed over quickly by those who, for example, don't need to review severe-storm dynamics, or who have already decided that a given mechanism is not a viable one.

With one exception, the processes I will discuss are all aerodynamic, that is, the waves radiate from the free motions of the air itself. It has long been suspected that the bulk of the acoustic-gravity wave energy in the atmosphere arises from aerodynamic sources, but the general theory of aerodynamic sound, in its present form (cf. Lighthill, 1962; Proudman, 1952; Stein, 1967), is difficult to apply to the specific atmospheric processes thought to be responsible. It is useful to examine aerodynamic sound from two viewpoints: one treats the emitting air flow stochastically, that is, as "turbulence"; the other seeks sound-generating air flows that can be modeled deterministically, or "exactly." I conclude that neither viewpoint alone yields a completely satisfactory model and that a hybrid model is required to explain the entire emission spectrum.

I begin in the following section by reviewing separately the particular aspects of convective-storm dynamics that are related to the acoustic-emission models I will discuss. Each of the proposed mechanisms will be introduced, but quantitative examination of each is postponed until the succeeding five sections. Table 1.1 summarizes the different kinds of acoustic sources to be considered. Section 8 is an assessment of the relative merits of all the models discussed, in which a most reasonable model is suggested. I also propose refinements to the model chosen and suggest some critical observational tests.

Table 1.1 Source Candidates

1. Simple sources in cumulus growth
   - A. Latent heat release (monopole)
   - B. Cell circulation (dipole)
   - C. Buoyancy oscillations (dipole)
2. Turbulence
   - A. Reynolds stress viewpoint (quadrupoles)
   - B. Random vorticity viewpoint
3. Electrical
   - A. Discharge shock (thunder)
   - B. Electrostatic relaxation
   - C. Pulse lengthening (nonlinear effects)
4. Vortex Sound
   - A. Aeolian tone (wake vortices)
   - B. Vortex instabilities (multiple vortices)
5. Heat-driven Oscillations
   - A. Combustion oscillations (periodic latent heat release)
   - B. Condensation in supersaturated environment

2. CONVECTIVE-STORM DYNAMICS FROM A WAVE-GENERATION VIEWPOINT

The existence of many reviews and monographs on storm dynamics and the abundance of research papers they cite make it unnecessary to present here a self-contained account of the subject (see for example, Byers and Braham, 1949; Newton, 1967; Atlas et al., 1963). Instead, this section highlights only those aspects of severe convective storms that seem germane to the problem of infrasound generation: (a) the dynamics of the convection currents inside storms, (b) the dynamics of the environmental flow in the storm's vicinity, (c) the nature and energetics of electrical discharges in a storm, and (d) energy release by condensation of water vapor. It will emerge that storm features with spatial scales of about a kilometer and temporal scales of tens of seconds are most likely responsible for the emissions. But because details of storm phenomena on these scales are virtually unknown, direct observational verification is not yet possible. Inferences about the smaller scale structure and motions of storms are drawn mainly from what we know about larger-scale features. The most suitable model will therefore be judged on the basis of realism, theoretical consistency, and conformity with the wave observations.

2.1 How Storms Begin

A convective or cumulus cloud forms when moisture-laden air rises above the level in the atmosphere where, because of adiabatic cooling, it can no longer retain all of its moisture content in vapor form. Water vapor condenses, usually on particulate (condensation) nuclei in the atmosphere, into cloud droplets, some of which may continue to grow in size and eventually fall out of the cloud as precipitation.

Meteorologists have historically divided convective storms into two kinds, based primarily on the synoptic or large-scale conditions leading to their development: Relatively small, isolated thunderstorms, sometimes called the air-mass type, (Byers and Braham, 1949) grow from the amalgamation of many smaller convective plumes initiated by solar heating of the earth's surface. These storms involve only a single air mass, as opposed to frontal storms, which develop near the boundary between relatively cold and warm airmasses. Fundamentally, they represent the release of potential energy, by local overturning, of a conditional instability in the atmosphere. Conditional instability is created when synoptic-scale processes cause heavy (cool and dry) air to overlie a layer of lighter (warm and moist) air.

Storms occur only when overturning gives rise to the condensation of a sufficient quantity of atmospheric water vapor. When condensation begins, the release of the water's latent heat of vaporization drastically alters the energetics of the overturning; the increased buoyancy provides positive feedback that amplifies the overturning until some external limit (such as moisture supply) stops it. When and where air-mass storms develop on a synoptic

scale are determined mainly by situations that supply moist air at low levels, but on a local scale, their development is controlled by nonuniformities in surface heating, by topography and by mesoscale atmospheric wave motions. Furthermore, storm development is inhibited by elevated temperature inversions. Because these mesoscale (10-100 km) controlling factors are poorly resolved on the synoptic scale, the specific times and locations of air-mass thunderstorm outbreaks are very difficult to predict.

But most very large and severe thunderstorms occur near synoptic-scale fronts or boundaries between air masses. The classic pattern is typical of the Great Plains in the spring and summer: A tongue of warm, moist Gulf air pushing northward at low levels encounters a mass of cool, dry air flowing south-eastward. The giant Great Plains thunderstorms form near the interface (or front) between the two air masses. Frontal storms are generally more severe than the air-mass type because there is additional dynamic support leading to deeper, more vigorous, and more organized convection. Such thunderstorms often form continually in squall lines that parallel the front and are pushed ahead of the front as it moves. The majority of storms that have been identified as strong infrasound emitters appear to be of this latter, more intense frontal type.

2.2 How Storms Develop and Intensify

The intensity or severity of thunderstorms has been found empirically to depend on the amount of moisture available at low levels, the amount of conditional instability in the atmosphere, and the vector shear (vertical gradient) of horizontal winds. Once a dynamical mechanism releases the instability, the positive feedback of latent-heat release during water phase changes provides the fuel for continued buoyancy and growth, accounting for most of the total energy released in a large thunderstorm. Following the onset of precipitation, certain storms experience an almost explosive growth into the great anvil-topped cumulonimbus that penetrates the tropopause.

Even at this early stage in our discussion of storm dynamics, we can envision two possible infrasound-radiation mechanisms. Our experience with the noise from explosions of all kinds suggests an analogous process, but on a longer time scale, associated with the explosive energy release that causes rapid cloud growth. In other words, we want to ask whether a developing cumulonimbus looks acoustically like a "slow explosion," with its radiated frequency and efficiency lowered. To find out, we can represent the release of latent-heat energy in a storm by an acoustic monopole and calculate the acoustic energy radiated by a local injection of fluid energy equivalent to that released in condensation. This estimate will be carried out in Section 3.1. We will conclude that the required acoustic power is available from a monopole mechanism, but that there is no evidence that the mechanism is effective in the required infrasonic frequency range. Much of the radiation from cumulus growth probably goes into atmospheric gravity waves.

The combination of convection and the release of latent heat in storms also suggests another class of sound-emitting processes that could arise from a resonant coupling between the two. Thermomechanical or heat-driven oscillations are well known in certain combustion systems, for example, rocket engines and gas furnaces. Rayleigh (1878) recognized that if an oscillating heat source has a component of its rate of heat release in phase with an acoustic density oscillation, then the acoustic oscillation will be amplified. For amplification to occur, the heat-release process must depend on the pressure, density, or flow velocity, and acoustic energy must be fed back to the heat source in proper phase. Feedback can be either direct acoustic feedback, as when, for example, the heat source is enclosed in an acoustic resonator, or by means of the flow that passes through the heat source. In Section 7 we will see whether any such mechanisms are relevant to infrasound generation in convective storms.

2.3 Air Circulation in Storms

Even though, for historical and forecasting purposes, air-mass and frontal may be convenient storm classes, they are inappropriate for the classification of specific kinematic and precipitation structures. Though differing perhaps in size and intensity, air-mass and frontal storms can and often do go through similar stages of development with nearly identical structural appearances. It is therefore more appropriate to use a classification system based on the concept of a precipitation cell. This scheme has emerged with the advent of weather radars. Such devices have the capability of resolving the fine structure ($\sim$ 1 km scale sizes) of precipitation content — strictly radar reflectivity. Small regions of relatively high reflectivity are identified with individual convective elements or cells and constitute the basic building block of convective storms. Two kinds of cells commonly referred to are ordinary cells and supercells (a term first introduced by Browning (1964) and applied to severe storms consisting of a single large cell).

Most storms are composed of one or more ordinary cells. These cells are relatively short-lived and evolve through three stages identified by Byers and Braham (1949) as: the cumulus stage (with updrafts alone), the mature stage (with updrafts and downdrafts coexisting), and the dissipating stage (with downdrafts throughout). Ordinary cells have a lifetime of about an hour, with a mature stage of only 10 to 15 minutes. Thunderstorm complexes can be composed of several such cells at various stages of development (Chalon et al., 1976). A disorganized, nearly random collection of these cells typifies the air mass thunderstorm. An organized succession of cells, on the other hand, is more typical of frontal storms. A recent kinematic model of an organized, multicell hailstorm has been presented by Browning et al. (1976) and is shown in figure 1.

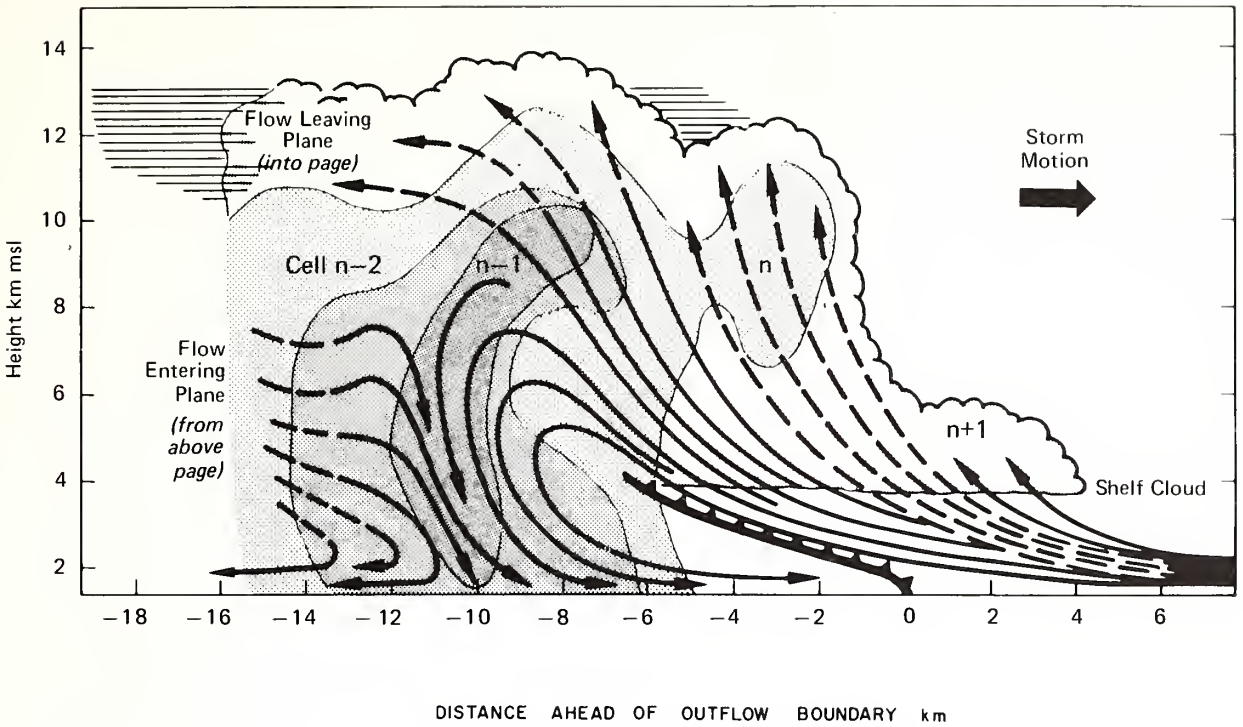

Figure 1. Schematic model of an organized multicell hailstorm, showing a vertical section along the storm's direction of travel through a sequence of evolving cells. Solid lines are streamlines of flow relative to the moving system; they are shown broken on the left side of the figure to represent flow into and out of the plane and on the right side of the figure to represent flow in a plane a few kilometers closer to the reader. The cells are numbered as follows: n+1 = growing cumulus; n = first radar echo; n-1 = mature; n-2 = decaying (after Browning et al., 1976).

In the presence of large conditional instability in the surface layer capped by relatively dry, potentially cold air in the middle levels and accompanied by strong wind shear (usually veering with height of the horizontal winds), a much more intense and longer lived convective element, the supercell, will develop. The important features of a supercell which travels to the right of the middle tropospheric winds are described by Browning (1964) and summarized in Figure 2. Such a storm often exists in a quasi-steady state for one to several hours.

In view of the frequency range of the acoustic waves whose source we seek (tens to hundreds of seconds wave periods) we now focus our attention on the shorter term fluctuations in storm airflow instead of on the longer scales appropriate to a storm's life cycle.

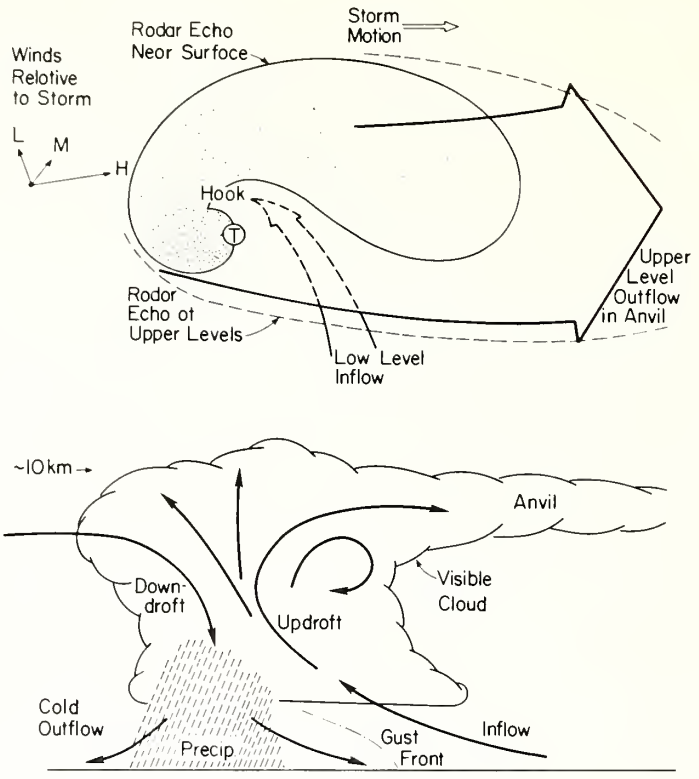

Figure 2. Plan view (upper) and vertical section (lower) of a model of a severe local storm that travels to the right of middle-level tropospheric winds. Stippling in the plan view is proportional to precipitation intensity; arrows indicate the main features of the airflow believed to be common to all such storms. The circled T shows the most likely place for tornado formation. (After Browning, 1964).

There is substantial evidence that cumulus growth in convective storms is not always steady but sometimes occurs in bursts (cf. Letzman, 1930; Workman and Reynolds, 1949; Abe, 1923; Priestley, 1953). In multicellular storms, the successive emergence of individual convective cells at cloud top in a succession of visual cloud towers often presents a pulsating appearance (Scorer and Ludlam, 1953). Anderson (1960), in a photographic study of five orographic cumuli in Arizona, found clear evidence of a 10-min periodicity in cell growth, superimposed on which were smaller, shorter period "turbulent" fluctuations. He concluded that cumulus growth is a superposition of an oscillatory type of cellular motion upon a steady growth, even for smaller cumuli that do not develop into thunderstorms.

Newton (1966) has used radar to study the pulsations of the cumulus towers of an Oklahoma squall-line storm that penetrated the stratosphere. He explains the observed alternate inflation and deflation of towers as the damped oscillation of an updraft parcel as it experiences negative buoyancy as it overshoots into the stable stratosphere and then a positive buoyancy as it

returns to the troposphere, having been warmed by mixing with environmental air. The oscillation is damped by form drag and entrainment of environmental air. Judging from his sequence of radar storm profiles, the oscillation period is roughly 15 min.

Turner (1966) has suggested that buoyancy oscillations are controlled more by evaporative cooling at cloud top, which reverses the buoyancy of a thin cloud-cap layer. His laboratory experiments with buoyant plumes of salt solution reveal violent and regular oscillations as mixing with their environment reverses their buoyancy. For typical cloud parameters, he predicts an oscillation period of 15 min.

Note that two different kinds of pulsating motion in cumulus growth are now proposed: One involves oscillations about the level of neutral thermal buoyancy of individual air parcels (which probably experience mixing with the environment, however); the other involves the successive (non-oscillatory) emergence of separate larger convective cells at cloud top. The former (oscillatory) mode should occur to some extent within every buoyant element, and thus constitutes a small-scale (turbulent) motion superimposed on nearly all convective storms. The latter mode, however, is characteristic of non-steady multicellular storms.

The distinction between steady and non-steady storms is not precise; in fact, at different times in the life of a storm, either steady or pulsating modes of convection may occur. Newton (1963) says that a pulsating convection mode appears to be favored in growing cumuli before downdrafts develop, whereas forced convection, in which strong downdrafts play a lifting role, appears to favor steady flow. A significant number of storms may be of an intermediate character, that is, having a "pulsating steady" updraft in the sense that a connected column of rising air has bursts of more intense convection superimposed on it. This sort of behavior seems to be the basis of the suggestion by Pierce and Coroniti (1966) that buoyancy oscillations in growing cumuli act like a piston to generate acoustic-gravity waves that reach the ionosphere with detectable amplitude.

All of these facets of a time-varying circulation pattern in convective storms suggest a single acoustic radiation model: an acoustic dipole. An incompressible toroidal flow resembling the central updraft and surrounding downdraft of a single convection cell can be reproduced by the velocity field of a fluid-dipole distribution on a horizontal, disk-shaped surface, with fluid sources on top and sinks on the bottom. Changes in the strength of such a dipole source would be communicated instantly to all parts of an incompressible medium. In a compressible flow with low Mach number, the velocity field of such a source remains virtually the same as in incompressible flow, but changes in source strength radiate into the medium as acoustic energy. Thus, by representing fluctuations in updraft strength in convective storms as the field of a distribution of varying acoustic dipole sources, we could estimate the radiated acoustic energy and its spectral content. The same acoustic problem can be alternatively formulated in terms of changes in the strength of a ring vortex, or as the radiation from a vertically accelerating air-mass. In our calculations, we use the last method.

The oscillations we have been discussing need not be monochromatic. It has been suggested that an air parcel undergoing buoyancy oscillations at the local Brunt frequency might emit compression waves at twice that frequency because the oscillating parcel displaces adjacent air back and forth horizontally twice for every vertical parcel oscillation. Furthermore, vertical variability of the local Brunt frequency could cause non-sinusoidal oscillations with high harmonic content.

2.4 The Role Environmental Winds Play

Early concepts of thunderstorm development held that strong vertical wind shear diminishes a storm's intensity by destroying its updraft. However, following the Thunderstorm Project in 1948 and 1949, researchers soon established a strong correlation between storm severity and strong middle-level winds. Specifically, Fawbush et al. (1951), after studying many tornado-spawning storms and their environments, found as a necessary condition on the synoptic scale the presence in the middle troposphere of a jet of strong winds exceeding 35 knots (18 m s^{-1}). Strong middle-level winds also consistently accompany the most severe and long-lived hailstorms. Newton and Newton (1959) established the same behavior for intense thundery rainstorms. Ludlam (1963, his Fig. 5) shows a remarkable coincidence between the geographic distribution of severe hailstorms and thundersqualls and the mean position of the 500 mb jet axis during the months in which the storms occur. On the basis of this evidence, the existence of a strong middle-level jet is now regarded as an essential ingredient for transforming a short-lived thunderstorm to one that persists for up to 12 hours or more and may travel several hundred miles. Perhaps such a jet is the ingredient that also transforms an ordinary thunderstorm into an infrasound emitter.

The reason given for storm intensification by wind shear was that a storm exposed to changing winds at different levels has its supply of moist air continually replenished, whereas a storm in a stagnant environment soon runs out of "fuel".

In an effort to quantify the dynamical interaction between a storm and its environment, Newton and Newton (1959) constructed a cumulonimbus model in which, for the first time, wind shear plays the role of intensifying and prolonging convection, and causes continual cell regeneration on the storm's forward right flank. Because strong convection effectively destroys vertical shear within the cloud (and not vice versa), the incloud air assumes a horizontal velocity intermediate between the ambient wind at upper and lower levels. Through its ability to resist environmental shear, the storm now acts as an obstacle in the flow and dynamic pressures are exerted on the storm boundary, positive on the upstream side and negative on the flanks and downwind side (Fujita and Arnold, 1963). These dynamic pressures convert a portion of the mean flow's kinetic energy to kinetic energy of the storm's vertical motions as discussed in detail by Newton (1967).

A possible relevance of the storm-environment interaction to sound generation lies in the role of large storms as obstacles in the environmental flow. An analogy with our everyday experience is again suggested: wind blowing around obstacles such as buildings, trees, and wires produces familiar sounds. The nature of these sounds is determined by the structure of wakes generated in the flow by the obstacles. We want to know whether severe storms also produce wakes and, if they do, whether low-frequency sound is emitted.

Fujita and Arnold (1963) have reported wind-field measurements in the vicinity of a Kansas thunderstorm that clearly show environmental wind maxima on the flanks of the strong-echo core of the storm, in direct analogy with the flow pattern observed in laboratory flows past cylindrical obstacles. As early as 1962, Fulks hypothesized the existence of thunderstorm wake vortices and a possible relation to tornado generation, but little evidence has emerged to support an association with tornadoes. Even if wake eddies are not directly involved in tornado genesis, there is evidence that significant amounts of the momentum of the mean flow are converted into local concentrations of vorticity in or around a storm, and at least contribute one ingredient favoring tornado development. Recent radar observations (Jessup, 1972; Brown and Crawford, 1972; Lemon, 1976) confirm the role of a thunderstorm as an obstacle in the flow and suggest that the wake of a storm updraft contains vortex tubes of cumulus scale. But none of these observations tells us much about the dynamics, the life cycles or the ultimate fate of wake vortices or other details of cumulus wakes that may be invisible to radars because they exist outside the storm cloud.

One possibility is that some vortices break free of the storm-obstacle, travel downstream like ordinary wake eddies, and decay according to ordinary two-dimensional models for the diffusion of vorticity (cf. Wilkins, 1970). Alternatively, the same instability that causes the storm itself may play a role in sustaining convection in shed eddies, possibly causing them to develop into self-sufficient storms (cf. Fujita and Grandoso, 1968). A third possibility is that wake eddies remain bound to the parent storm and become integral parts of its circulation, as suggested, for example, by Jessup (1972) and by Eagleman (1971). In this third case, it may be less useful to view the phenomenon as a wake eddy than simply as a portion of the environmental flow that becomes part of a helical downdraft, perhaps intertwining with an updraft, as sketched in the paper by Browning (1964). Lemon (1976) , for example, has suggested that some wake vortices may be related to the "starting vortices" of airfoil theory, balancing the equal but opposite vorticity in a storm's rotating updraft.

Consequently, we are not sure whether to model storm wakes as fully turbulent or as regular Karman vortex trains. Both kinds of wakes can emit aerodynamic sound, but different approaches are used to analyze them. Periodic wakes can best be described in terms of a regular vorticity distribution, whereas fully turbulent wakes have to be modeled stochastically.

A special case of wake-generated sound is the aeolian tone, in which the Reynolds number of the flow is in the proper range for the wake to be composed of a highly periodic train of vortices that have been shed from the obstacle.

Nearly monochromatic sound is emitted at the eddy-shedding frequency. The aeolian harp and the singing telephone wire are classic examples. That similar vortex trains exist on mesoscale and larger has been confirmed by satellite photographs of the wakes behind certain islands (Chopra and Hubert, 1964a, 1964b; Zimmerman, 1969; Chopra, 1973). Either the warm-air bubble that sometimes forms over an island or its mountains diverts the flow horizontally around the island when a suitable temperature inversion prevents much vertical flow diversion. The same inversion often provides a cloud layer that makes the resulting flow perturbations visible on satellite photographs. Similarly, as a storm approaches the tropopause, diversion of the environmental flow should become mainly horizontal because vertical deflection is inhibited by the static stability of the stratosphere.

In Section 6.3.2 I estimate the sound that could be radiated by wakes that thunderstorms might produce. I conclude that the aeolian-tone mechanism could radiate the required acoustic power, but the sizes of the wake eddies that seem to exist would radiate at frequencies lower than those observed.

2.5 Vorticity Inside Storms

The most significant single clue to the origin of severe-weather infrasound is its close association with tornadic storms in the Midwestern U.S. Specifically, in a recent study of infrasound received at Boulder, Colorado, during an entire storm season, 45 of the 86 storms that were identified as infrasound sources produced documented tornadoes or funnel clouds (Georges, 1973; Georges and Greene, 1975). The 45 tornadic storms were a small fraction of all the storms that occurred in the Midwest during the observing period, yet they constituted a majority of the infrasound emitters. Furthermore, it is easy to imagine various difficulties with the tornado-reporting system, such that tornadic (or at least pre-tornadic) activity was indeed present in many or even all of the remaining 41 infrasound-emitting storms, but was not observed or reported for any of several reasons (unpopulated area, nighttime, tornado obscured by cloud or precipitation). Because of this compelling observational evidence, storm mechanisms associated with tornado production, and specifically those that give rise to concentrations of vorticity in storms, deserve special attention as potential infrasound generators.

There is no a priori reason for believing that only fully developed tornadoes emit infrasound. Indeed, comparisons of the details of timing and duration of observed infrasound with tornado reports suggest that such is <u>not</u> the case. Although observations are sparse, there is evidence for the existence of a larger class of storm-associated vortices, some of which are related to tornado genesis, but others of which grow and die unseen, either entirely within a storm cloud or in the clear air surrounding it. It is this broader class of vortex phenomena whose dynamics and infrasound-generating potential we now examine.

Portions of large convective storms exhibit rotation great enough to be observed visually (especially in time-lapse photography) and in their radar echoes. The nature of this kind of rotation is evident from the flow pattern depicted in Figure 2; the low level inflow makes a roughly 270° turn as it convects upward through the storm and is expelled at the top. Brown et al. (1971) have suggested that the "hook" echoes seen on weather radars are probably distortions of the precipitation echo by such rotating updrafts. The relevance of hook echoes to tornado genesis is thus reasonable (Fujita, 1973). Rotation in storm downdrafts has also been suggested (Eagleman, 1971), but the evidence for its existence is less substantial.

Doppler radars have revealed the existence of mesoscale vortices (whose solid rotating cores are 5 km or so diameter) inside some tornadic storms (Kraus, 1973; Brown et al., 1973) as well as in non-tornadic storms (Figure 8 and Kropfli and Miller, 1975, 1976). Evidently, such rotations are characteristic of many kinds of convective storms.

As this and the preceding section suggest, there is no shortage of indications (both theoretical and observed) that storm-scale vorticity exists in profusion inside and in the vicinity of thunderstorms. Yet, on the next scale smaller than that of the storm itself, that is, less than a kilometer, practically no information about vorticity distribution exists. These are the scales of motion that are the most likely sources of the observed acoustic radiation.

We have two choices with regard to modeling these motions and estimating their acoustic radiation: First, in the absence of a deterministic spatial and temporal description of the vorticity field, we could resort to a stochastic description and use measured values of the turbulent velocity fluctuations inside storms. The acoustic radiation from homogeneous, isotropic turbulence has been modeled, for example, by Lighthill (1952, 1954, 1962), Proudman (1952) and Morse and Ingard (1968). This method only marginally meets the radiated-power requirements imposed by the observations; furthermore, some of the assumptions about spatial and temporal stationarity implicit in the turbulent model are not satisfied by storm-related air motions.

Our second choice is to calculate the acoustic radiation from simple time-varying vortex configurations. As examples, I chose a corotating vortex pair and the vortex-shedding process responsible for aeolian tones. The aeolian-tone mechanism could produce the required radiated power, but again, the frequency range, for realistic storm parameters, is too low. I find that the corotating vortex mechanism could be effective at the observed frequencies and could emit the required power under conditions observed in the most severe storms. Furthermore, by invoking a multiplicity of such sources in various stages of growth and decay, the nonstationary nature of the observed radiation could be duplicated.

2.6 Thunderstorm Electricity

The exact mechanism of charge separation and the details of electric charge distribution in thunderstorms are still under active debate. The most commonly suggested mechanisms suppose that charges of opposite sign attach to particles that, because of size differences, move at different velocities relative to the rising air stream of a storm's updraft. When a large enough potential difference is built up between different parts of a cloud, or between a cloud and the ground, an electrical breakdown of the intervening air takes place in a series of steps that culminates in a massive electrical discharge arc.

Fortunately, the aspects of thunderstorm electricity that could be relevant to infrasound generation do not seem to depend critically on these details. The reader interested in the subject should consult the books by Uman (1969) and Chalmers (1967) and the many references they cite. We will confine our attention to events associated with the electrical (lightning) discharge.

The obvious relevance of lightning to infrasound generation lies in the possibility that the infrasound is simply low-frequency thunder. But the results of numerous measurements of the acoustic spectrum of thunder (Few et al., 1967; Bhartendu, 1971; Few, 1969; Holmes et al., 1971) indicate that there is not nearly enough acoustic energy in the infrasonic portion of the spectrum to explain the observed infrasound intensities. Only the possibility that the spectral content of thunder may be shifted into the infrasonic range by nonlinear pulse-stretching in the upper atmosphere prevents us from immediately discarding thunder as a reasonable source candidate. In Section 3.3 I examine the pulse-stretching mechanism, and the evidence that it actually occurs in the atmosphere, to see if it could quantitatively explain the observed properties of severe-weather infrasound.

I also examine a suggestion by Dessler (1973) that electromechanical relaxation inside thunderstorms following lightning discharges radiates detectable infrasound. The basic idea is that in charged regions of a thundercloud, charged water droplets repel each other and set up a region of locally reduced pressure. When the charge distribution is suddenly neutralized by a lightning discharge, a sort of implosion occurs, radiating a rarefaction wave whose dominant frequency and intensity are determined by the size and shape of the emitting region. I raise several questions about the validity of such a model, and make more accurate estimates of the radiated acoustic energy. I conclude that the relaxation process, if it occurs, probably radiates infrasonic pulses, but that it is probably not the source of the severe-storm infrasound.

The following sections examine in detail the acoustic source mechanisms introduced in this section.

3. SIMPLE ACOUSTIC SOURCES

An acoustic monopole is used to model the acoustic radiation caused by local injections of fluid mass or energy. An acoustic dipole is used to model the acoustic radiation from local changes in fluid momentum. An acoustic quadrupole is used to model the acoustic radiation from local changes in fluid momentum flux. I now examine the appropriateness of each of these simple acoustic sources for describing processes known to occur within thunderstorms.

3.1 Monopole Source

Unless a fluid or energy source actually exists in a fluid, monopole radiation is very weak and any effective monopole radiation present is due to retardation effects in higher order sources that are not small compared with a wavelength (Morse and Ingard, 1968). In convective storms, energy is released inside the cloud by water-vapor condensation and sublimation. At the acoustic wavelengths of interest here (tens of kilometers), this source must account for virtually all monopole radiation from storms. We can make crude estimates of the total energy released and its duration, but spatial and temporal details of the release are not known. Therefore, we can estimate the average rate of acoustic energy radiation but cannot yet know anything at all about the higher-frequency (shorter wave period than the storm lifetime) radiation that may be caused by fluctuations in the energy-release process.

A crude but sufficiently accurate lower bound on the latent heat released in a severe rainstorm can be obtained by calculating the heat of vaporization of a storm's total rainfall. Suppose an average 5 cm of rainfall from a severe thunderstorm covers a ground area 10 x 10 km. The total water volume is 5×10^6 m^3, and its mass is 5×10^9 kg. Condensation releases 2.5×10^6 J kg^{-1}, so the total heat released is 1.3×10^{16} J.

This heat energy dh (per unit mass) is partitioned into (a) increasing the storm's internal energy (temperature) and (b) doing work, mainly expanding the air inside the storm (although small fractions go into changes in its kinetic and potential energies). Therefore

$$dh \simeq C_v dT + pdv, \tag{3.1}$$

where v is the specific volume of the gas, and C_v is its specific heat at constant volume. If we assume that this process takes place under nearly constant pressure, then we also have

$$dh \simeq C_p dT. \tag{3.2}$$

We can combine (3.1) and (3.2) to find out what fraction of dh goes into expanding the air:

$$pdv = dh\ (1 - \frac{C_v}{C_p}). \tag{3.3}$$

Recognizing that $C_v/C_p = 1/\gamma$ and letting $\gamma = 1.4$, we obtain, for the change of storm volume dV,

$$pdV = 0.29dH. \tag{3.4}$$

(Lower case letters refer to specific quantities per unit mass; upper case refers to total quantities in a storm.) So about one third of the heat goes into expansion. Using the 1.3×10^{16} J obtained above for dH and $p = 5 \times 10^4$ N m^{-2}, we get

$$dV = 7.5 \times 10^{10}\ m^3. \tag{3.5}$$

From the equation of state (with pressure constant) and (3.2) we obtain

$$\frac{dV}{V} = \frac{dT}{T} = \frac{dh}{C_p T}. \tag{3.6}$$

A typical mixing ratio inside a severe storm is up to 10 gm H_2O per kilogram of air, giving a latent heat release dh of about 2.5×10^4 J kg^{-1} of air, assuming all the vapor condenses. Using $C_p = 1005$ J kg^{-1} K^{-1}, we get for the fractional volume and temperature changes,

$$\frac{dV}{V} = \frac{dT}{T} = 0.09, \tag{3.7}$$

or almost 10 percent. Such a volume change occurs over the storm growth phase, nominally 1000 s.

The spectral content of the acoustic radiation depends on the exact form of V(t), the temporal behavior of the expanding volume; if it is smooth, the emissions will contain mainly the frequency characteristic of the storm growth time. Higher frequencies would be generated by fluctuations in volume change (caused, for example, by fluctuations in heat release) superimposed on the overall storm growth.

I now estimate an upper bound for the acoustic energy contained in monopole radiation at various high frequencies. Let V_m be the total volume change (caused by latent heat release) that occurs during the storm-growth time T. Suppose volume fluctuations of shorter period T' are superimposed on this growth, but impose the additional condition that V must increase monotonically with time (this means that heat is not periodically fed back to evaporate water droplets; we will discuss this possibility separately in Sec. 7). The amplitude of volume fluctuations at wave period T' cannot be much larger that $\frac{T'}{T} V_m$. The time rate of change of volume at period T' is thus of the order of $\frac{1}{T'} \frac{T'}{T} V_m$, or just the same as the average rate of change of volume. With

the value of V_m given in Eq. (3.5) and a 1000-s lifetime, we get an average volume rate of change

$$S = \frac{dV}{dt} \simeq 7.5 \times 10^7 \text{ m}^3 \text{ s}^{-1} . \tag{3.8}$$

Morse and Ingard (1968, Sec. 7.1) give the following formula for the rms acoustic radiated power Π from a monopole source of strength S_ω at frequency ω

$$\Pi = \frac{\rho\omega^2}{4\pi C} |S_\omega|^2 , \tag{3.9}$$

where C is the speed of sound and ρ is the air density. Leaving the wave frequency ω variable for the moment, and using values appropriate to the troposphere, we get (in mks units)

$$\Pi = 1.6 \times 10^{12} \omega^2 . \tag{3.10}$$

If all the energy were radiated at a wave period of 30 s, for example, ($\omega = 0.209 \text{ s}^{-1}$) $\Pi = 7 \times 10^{10}$ W. This is at least two orders of magnitude larger than the infrasonic wave observations require.

At the present time, there is no theoretical or observational reason to believe that such coherent higher frequency fluctuations in latent heat release actually occur. All we have shown is that such fluctuations could easily account for the observed wave intensities. Arguing against coherent fluctuations in latent heat release over such a large volume is the fact that the typical storm size is about an acoustic wavelength at tens of seconds wave period. A fluctuation in one part of a storm would change phase substantially before its effects could be communicated acoustically across the storm.

3.2 Dipole Source

Not all the motions inside a storm are caused directly by the release of latent heat of vaporization; we can conceptually separate the fundamentally expansive motions, which we represented by an acoustic monopole, from the cellular or (ideally) toroidal convection pattern caused partly by the static instability of the atmosphere and reinforced by latent heat release. I now estimate the equivalent acoustic dipole strength using measurements of thunderstorm updraft speed and size, but again, the spectral content is unknown on time scales shorter than the storm's lifetime.

There are several practically equivalent ways to model the idealized convection pattern of a thunderstorm that would permit us to estimate its dipole radiation. First, we could assume a sphere, or bubble, of fluid accelerating vertically; second, we could assume a thin horizontal disk with varying fluid dipole sources distributed over its surface; or third, we could use a horizontal vortex ring whose strength varies with time. All three methods yield essentially the same hydrodynamic flow field and the same acoustic radiation for a given spectral content of the source variable. I use the first method for a sample calculation.

Morse and Ingard (1968, Sec. 7.1) give a formula for the acoustic power Π radiated by a sphere of radius $\underline{a}$ oscillating up and down with a frequency ω and maximum speed U:

$$\Pi = \rho C(4\pi a^2) \frac{(ka)^4}{12} U^2 , \tag{3.11}$$

where $k = \omega/C$. Evaluating the constants in mks units for the troposphere

$$\Pi = 3.2 \times 10^{-8} a^6 \omega^4 U^2 \text{ Watts.} \tag{3.12}$$

For $\underline{a}$ = 2.5 km, U = 10 m s^{-1} and a wave period of 30 s, $\Pi = 1.5 \times 10^{12}$ W. If we take the estimate of the average broadband acoustic radiated power required by the infrasonic measurements, about 10^8 to 10^9 W, and the same values for $\underline{a}$ and ω, we require velocity fluctuations of only 0.08 to 0.25 m s^{-1} at 30 s period, not unreasonable for fluctuations in thunderstorm updrafts. Note, however, that the model requires the fluctuations to be coherent over a sphere of radius $\underline{a}$. If we decrease the value of $\underline{a}$ by a factor n, the required U increases by a factor of n^3.

The remarks at the end of the last section can be paraphrased here: a dipole source appears to be quantitatively realistic only if coherent motions of the required amplitude exist at the proper frequencies. Again, supporting experimental data are lacking.

3.3 Quadrupole and Higher-Order Sources

I could extend the discussions of the preceding sections to calculate the radiation from higher-order simple sources; however, this would probably serve no useful purpose, because no identifiable storm processes suggest description by such sources, and because the same problems arise with respect to the energy in higher-frequency fluctuations.

Models of sound radiation by turbulence employ a random-quadrupole representation of fluctuations in Reynolds stresses in fluids, and this stochastic approach will be examined next.

4. TURBULENT SOURCES

From the point of view of acoustic radiation, it is useful to divide fluid motions into three kinds: (a) steady, or time-invariant, flows, (b) nonsteady flows of low Reynolds number, whose principal dynamic features can be described "exactly," and (c) nonsteady flows of high Reynolds number that are too chaotic to be described deterministically. That steady flow radiates no sound is obvious, for example, from energy considerations, and it is therefore of no direct interest to us. The sections on simple sources and on vortex sound contain examples of nonsteady flows that are modeled in an exact way, and whose radiated sound is exactly determined from the flow field. The third kind of flow, which we can at present describe only in terms of its statistically averaged properties, is called "turbulence." Turbulent flows also radiate sound, but because the flow is described only statistically, the sound field, too, is described only in statistical terms.

The airflow inside severe thunderstorms indeed defies exact description and so qualifies for the label "turbulent"; yet certain gross storm features seem to fit deterministic models for convective flow, and so in some sense can be considered "known." (It is, in fact, a steady migration of storm characteristics from the former category into the latter that measures what we call an increased "understanding" of storms.) Yet it appears that storm airflow will never be describable in detail, and that the ultimate storm model will be some deterministic description of storm-scale flow, upon which are superimposed smaller-scale "turbulent" fluctuations, whose influence is parameterized only in statistical terms. The question we face here is whether the deterministic part or the random part of storm motions, or some combination of both, is required to explain the observed acoustic radiation. To answer this question, I next examine the predictions of a turbulent-source model. A turbulent description of the severe-storm radiation mechanism is not very rewarding from the point of view of insight into storm processes, but it can be used to estimate average radiated power and the average acoustic spectrum when no exact description is possible.

To construct a simple turbulent description of severe-storm air motions, suppose that energy is supplied to the storm's motions (by convective instability) on an "outer scale", L, equal to the scale of the convection cell itself. According to the Kolmogorov hypothesis (Lumley and Panofsky, 1964), motions on smaller scales merely partake of an energy-cascade process that transfers energy to smaller and smaller scale motions, until an "inner scale" is reached where energy can be efficiently dissipated by molecular viscosity. In the in-between, or so-called inertial range of scales, where energy is neither supplied to nor removed from the fluid motions but is merely transferred by means of nonlinear interactions between scale sizes, the statistical and spectral properties of the turbulence (and its radiation) do not depend on the geometry of the driving mechanism.

Turbulence in the inertial range is said to be homogeneous and isotropic, properties that simplify its analysis and the calculation of its acoustic radiation. From dimensional arguments, it is possible to establish that the frequency spectrum of the (squared) pressure fluctuations in such a fluid

exhibits an $f^{-7/3}$ behavior (Lumley and Panofsky, 1964), but that the power spectral density of its acoustic radiation falls off with frequency as $f^{-7/2}$ (Morse and Ingard, 1968, Sec. 11.4; Meecham and Ford, 1958). If L is the largest scale of fluctuations in the storm we expect the radiated power spectrum to level off at a wave frequency of about $U_L/2\pi L$, where U_L is a representative velocity fluctuation on the scale L and then to fall off again at lower frequencies. For the largest thunderstorms, $U_L \simeq 30$ m s^{-1} and $L \simeq 10$ km, which give a wave period of about 30 min. So, it seems reasonable to hypothesize a wave spectrum for thunderstorm radiation that peaks in the vicinity of 20 to 30 min (actually, these would be gravity waves) and falls off at lower and higher frequencies, with the high-frequency falloff approaching an $f^{-7/2}$ rate. Meecham and Ford predict a low-frequency spectral density proportional to f^4.

For frequencies near the peak, however, the assumptions of a turbulent description (i.e., that the flow is of sufficient spatial and temporal extent to permit valid averages to be taken) break down. There, we would expect deterministic descriptions of the radiation to be more appropriate, for example, the acoustic monopole and dipole models described in Sec. 3, applied to scales of size L. A complete storm radiation model might then consist of a turbulent description of the high-frequency radiation, matched with a deterministic description of lower frequency radiation based on known storm motions.

To estimate the amount of acoustic power that could be radiated by turbulent motions of the intensity thought to occur within thunderstorms, I use an approximate formula derived by Proudman (1952), based on Lighthill's (1952) theory of acoustic radiation from homogeneous, isotropic turbulence. Lighthill's hypothesis was that the sound radiated from a region of turbulent fluid isolated from external forces is equivalent to the sound radiated by a random distribution of incoherent acoustic quadrupoles whose strength is related to the fluctuating stress field in the fluid. In air, on the scales of motion of interest to us, the principal form of fluid stress is not the "real" or viscous stress exerted across a fluid element by molecular motions normal to its boundaries; instead, distortions of fluid elements can be thought of as caused by Reynolds stresses - that is, by momentum ρu_i carried across the boundaries of a fluid element by fluid motion u_j. Because such stresses in a fluid tend to distort the shapes of fluid elements and cause them to rotate, one can think in physical terms of a distribution of point quadrupoles, located one per average eddy volume. The acoustic quadrupole strength is proportional to the strength of the fluctuating part of the Reynolds stresses.

The final result of Proudman's analysis (see also Morse and Ingard, 1968, Sec. 11.4) gives the total acoustic power Π radiated by a volume V of homogeneous, isotropic turbulence, in which there are rms Mach-number fluctuations M and a turbulent dissipation rate ε per unit mass:

$$\Pi = 38 M^5 \varepsilon \rho V \quad . \tag{4.1}$$

The value of ε indicates the intensity of turbulence and has been estimated inside thunderstorms from Doppler radar measurements (Strauch et al., 1975) to be between 0.1 and 1.0 $m^2 s^{-3}$; the latter value applies to the most severe storms, and we will use it. (Independent order-of-magnitude estimates of ε can be obtained using u^3/ℓ, where u represents velocity fluctuations on any scale ℓ.) We assume the largest reasonable value for the storm volume, V, a 10 km cube, even though we recognize that the assumed values of ε and M are maximum values and are not maintained over the whole storm volume. Using a value of 0.03 for M (about 10 m s^{-1} velocity fluctuations) gives $\Pi = 9.2 \times 10^5$ W; a value of 0.1 for M (about 34 m s^{-1} velocity fluctuations) gives $\Pi = 3.8 \times 10^8$ W.

As mentioned earlier, this power should be distributed (on the average) over a spectral region beginning at about 30-min wave period, with a power spectral density that falls off toward higher frequencies, ultimately approaching an $f^{-7/2}$ power-law slope. The total effective width of the emission spectrum seems to depend on the shape of the spectrum in the transition region between the frequencies corresponding to the outer scale and those scales that can be considered fully in the inertial regime. If the transition takes place in a decade or less, the total emission spectrum would appear quite narrow; with an $f^{-7/2}$ falloff, more than 80% of the power appearing above any given frequency is concentrated in the octave immediately above that frequency. The power density at the higher frequencies of interest to us would then certainly be inadequate. On the other hand, if the transition takes several decades, the spectrum could still be relatively flat at wave periods of tens of seconds. But then the results for radiation from the inertial range would not apply. I see no way to predict the spectral extent of the transition region on theoretical grounds alone; new storm observations, such as those now being made with dual-Doppler radars, may help answer this question.

There are so many uncertainties associated with the turbulent-source model that it is not now possible to accept or reject it conclusively as a viable explanation for the observed emissions. Order-of-magnitude uncertainties exist in formulas like Equation (4.1) as well as in those describing the spectral properties of the emissions. Large uncertainties also exist in the storm parameters I assumed, because they have not yet been measured accurately or extensively. Only by using values for M, ε, and storm volume that are probably all larger than those actually present, even in the most severe storms, can we obtain values for the acoustic radiated power that come close to the measured estimates.

I conclude that a purely turbulent description of the emission mechanism is probably inadequate. I think that its main shortcoming is that it assumes a random distribution of incoherent sources, whereas there appear to be storm processes, vortex motion for example, that could produce coherent fluctuations over scales substantially larger than u/f, where f corresponds to the radiated frequency and u is the fluctuation velocity at that frequency. Infrasound waveforms that often exhibit many apparently coherent wave cycles also provide evidence against a purely stochastic viewpoint.

5. ELECTRICAL SOURCES

5.1 Lightning

One obvious source of sound in severe storms is thunder, the acoustic remnant of the shock wave generated by electrical discharges (lightning). It could reasonably be argued that, whereas the audible portion of the thunder spectrum is attenuated by ordinary absorption in distances of a few tens of kilometers (as is observed), an infrasonic portion (if one exists) would travel unheard with low loss to hundreds or thousands of kilometers. I thus ask first whether the acoustic spectrum of thunder extends to infrasonic frequencies with sufficient intensity to explain the observations.

Holmes et al. (1971) have measured the mean total acoustic energy of 30 cloud-ground flashes as 6.3×10^6 J, and Remillard (1960) gives 4×10^7 J as the acoustic energy radiated by a typical flash. The most energetic flash measured by Holmes et al. had an estimated total acoustic energy of 17×10^6 J. These estimates apply to the smaller, isolated thunderstorms such as occur in the New Mexico area. Somewhat larger values may apply to Great Plains frontal storms, but no measurements seem to be available.

How much of this energy lies in the infrasonic portion of the spectrum? Few direct measurements of the infrasonic spectrum of nearby thunder have been attempted, but those available suggest a sharp falloff in power density below audible frequencies. For example, Few et al. (1967) used pressure sensors with essentially flat response down to 0.1 Hz and reported a sharp falloff in power density below 10 Hz. This and other similar spectra indicate that the total amount of energy below about 1 Hz is several orders of magnitude less than the total acoustic energy radiated. This would put the total acoustic energy per flash below 1 Hz at no more than about 10^3 or 10^4 J, hardly enough to account for the 10^8 to 10^9 W (J s^{-1}) of average broadband source power required by infrasonic observations (Part I). Furthermore, it is difficult to reconcile the impulsive nature of thunder with the observations of nearly continuous emissions, even from nearby storms, where propagation effects cannot disperse a pulse train.

I am aware of no attempt to measure the acoustic spectrum of thunder that has utilized instruments suitable for the portion of the spectrum (below 0.1 Hz) that the severe-weather waves occupy. In particular, the effects of wind noise increase rapidly at wave periods of tens of seconds, and rather elaborate noise-suppression techniques must be used. Therefore, the question of the infrasonic energy content of thunder must be considered open, although it seems unlikely that significant infrasound radiates from the lightning channel itself. Another mechanism has been proposed, however, for low-frequency acoustic pulse radiation during thunderstorm electrification.

5.2 Electrostatic Sound

Discussion is continuing in the literature about whether the sudden release of electromechanical stresses in clouds contributes to the infrasonic spectrum of thunder (Colgate and McKee, 1969; Holmes et al., 1971a, 1971b; Bhartendu, 1971; Dessler, 1973). In Dessler's model, electromechanical stresses build up as charged water droplets rearrange themselves inside a cloud to maintain a balance between the electrostatic forces (arising from charge separation) and the dynamic pressure each droplet experiences by its motion through the air. When the electrostatic field suddenly changes after a lightning discharge, each droplet adjusts its motion in response to the suddenly uncompensated pressure field in its vicinity. This motion radiates sound. In simple calculations, Dessler considers disk- and cylinder-shaped volumes of like-charged droplets, initially at rest but which begin to move apart by mutual repulsion. The resulting dynamic pressure field contains a region of reduced pressure at the center of the disk (or cylinder). In perhaps oversimplified terms, the moving droplets "sweep some air along with them, thus creating a disk-shaped region of reduced pressure." In these examples, a sudden neutralization of the charge distribution (by a lightning discharge) causes a momentary implosion that radiates an acoustic-rarefaction pulse.

In an actual thunderstorm, the charge distribution and the dynamics of droplet motion are probably drastically modified by the dynamical processes that produce and maintain charge separation, processes whose nature remain obscure. Therefore, the particular geometries treated by Dessler must be regarded as idealized and possibly unrealistic. Furthermore, Dessler did not calculate the acoustic energy radiated by the imploding volume; his estimates of signal amplitude (0.5 to 50 μbar) are actually estimates of the pressure deficit at the center of the volume and not the amplitude of the radiated acoustic wave.

5.2.1 A Model for Radiation From an Imploding Sphere

A more satisfactory estimate of radiated acoustic energy uses Lamb's (1945) result for the pressure disturbance radiated by a sphere of radius a with an initial overpressure Δp inside, which is released at $t = 0$. The loss of realism suffered from the use of a spherical volume (rather than the disk-shaped or cylindrical models Dessler uses) seems minor except possibly as it affects the acoustic radiation pattern.

Lamb shows that the density disturbance ρ' has the form

$$\rho' = \frac{\Delta\rho}{2} \frac{(r-Ct)}{r} , \qquad (5.1)$$

where $\Delta\rho$ is the excess density inside the sphere at time $t = 0$, C is the speed of sound, and r is the distance from the center of the sphere.

Assuming the initial state is isothermal and choosing a time $t = \frac{R_o}{C}$, at which the spherical disturbance has reached a radius $R_o >> a$, we obtain the classical N-shaped pressure disturbance (Figure 3):

$$p' = \frac{\gamma \Delta p}{2} \left(1 - \frac{R_o}{r}\right), \qquad R_o - a < r < R_o + a$$

$$p' = 0 \qquad , \qquad R_o - a > r > R_o + a \ , \tag{5.2}$$

where γ is the usual specific heat ratio. Evaluating (5.2) at $r = R_o \pm a$ gives the peak value of the pressure disturbance,

$$p'_{max} = \frac{\gamma \Delta p}{2} \frac{a}{R_o \pm a} \cong \frac{\gamma \Delta p}{2} \frac{a}{R_o} \ , \quad R_o >> a. \tag{5.3}$$

We expect the real initial pressure distribution to be continuous (i.e., smooth) across the sphere boundary, which would round off the sharp edges of the N-shaped disturbance somewhat. In the case of interest to us, Δp is negative, so the initial pressure disturbance would be a rarefaction.

To obtain the total energy radiated, E_r, we integrate the energy density $p'^2/\rho_o C^2$ over the spherical wavefront of radius R_o from $R_o - a$ to $R_o + a$:

$$E_r = \frac{4\pi R_o^2}{\rho_o C^2} \left(\frac{\gamma \Delta p}{2}\right)^2 \int_{R_o - a}^{R_o + a} \left(1 - \frac{R_o}{r}\right)^2 dr. \tag{5.4}$$

The value of the integral is $8a^3/R_o^2$, to second order in a/R_o, so that

$$E_r = \frac{8\pi a^3}{\rho_o} \left(\frac{\gamma \Delta p}{C}\right)^2 \ ,$$

which is independent of R_o (for $R_o >> a$), as it should be.

We can also estimate the acoustic radiation efficiency, η, of an exploding (or imploding) sphere by comparing the radiated energy with the work done in an adiabatic expansion of the sphere. For adiabatic processes, pv^γ = constant, where v is the specific volume of the gas. Logarithmic differentiation shows that

$$pdv = - \frac{v}{\gamma} dp. \tag{5.5}$$

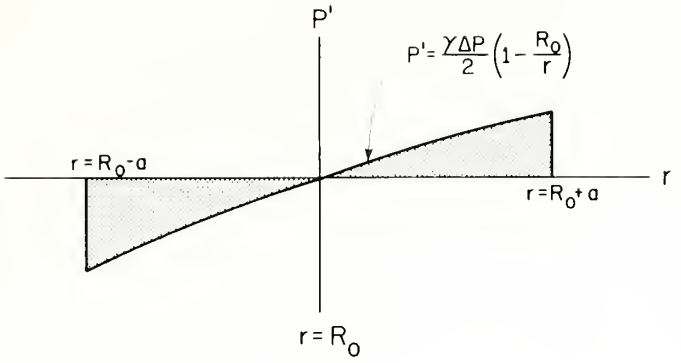

Figure 3. The pressure disturbance p' as a function of distance r radiated by a sphere of radius a and overpressure Δp, which is released instantaneously. For Δp negative, the rarefaction phase precedes the condensation phase.

The lefthand side is the work done, and if the fractional changes in p and v are small, the work done is

$$w = \int p \, d \, v \simeq - \frac{v}{\gamma} \Delta p \tag{5.6}$$

per unit mass. For the entire volume V,

$$W = - \frac{V}{\gamma} \Delta p, \tag{5.7}$$

where the minus sign indicates that, for Δp positive, work is done by the expanding volume on the surrounding gas. The ratio of E_r to W gives the radiation efficiency,

$$\eta = \frac{2\gamma^3}{C^2} \frac{\Delta p}{\rho_o} = 2\gamma^2 \frac{\Delta p}{p_o}, \tag{5.8}$$

since $C^2 = \gamma p_o / \rho_o$. The radiation efficiency is nearly equal to the fractional overpressure.

Using values appropriate to the electrostatic mechanism, I estimate the radiated acoustic energy, the acoustic efficiency, and the amplitude of the pressure wave. According to Dessler, the maximum value of Δp that can be generated by electrostatic forces is about 5 N m^{-2} (50 μbar). The radius of the volume is taken to be 5 km, about the same size Dessler uses. Other

constants are given the following values: $C = 340\ m\ s^{-1}$, $\gamma = 1.4$, $\rho_o = 1.2\ kg\ m^{-3}$. Then $E_r = 1.1 \times 10^9$ J. The radiation efficiency is 1.3×10^{-5}, and the peak pressure amplitude at a distance of 50 km is $0.35\ N\ m^{-2}$ or 3.5 μbar. These values probably represent the maximum possible field obtainable with this mechanism. At greater distances, the field strength falls off more slowly than the 1/r dependence given by (5.2), because of the ducting effects of atmospheric refraction.

5.2.2 Energy Comparison

By comparing this theoretical estimate of the maximum energy that could be radiated from a single electrostatic source of reasonable size with estimates of average radiated power based on severe-storm-wave observations (Part 1), we can infer a minimum rate of such emissions that would be required to explain the observations. The average broadband power radiated by the most powerful emitting storms was estimated in Part I as 10^8 to 10^9 W. If the electrostatic source model can emit no more than 10^9 J, such emissions every 1 to 10 s would be required to yield the observed average power flux. If the emission bandwidth of the actual waves is confined mainly to the observational "windows" (discussed in Part I), then a smaller average power flux and thus a lower emission rate would be required. On the other hand, if the size of the emitting volume or the pressure deficit inside it is smaller than the nearly maximum allowable values postulated in this estimate, then the radiated energy would be considerably smaller, and a much higher emission rate would be required. On an energy basis then, I conclude that the electrostatic mechanism is marginally satisfactory, but there are large uncertainties in the model, and to some extent in the observations, that make agreement highly tentative.

5.2.3 Spectral Considerations

To supplement the energy comparisons just made, I examine possible spectral discrepancies between model and observation. As in the radiation from the lightning stroke, the sound of electromechanical relaxation processes is essentially impulsive, depending on the lightning discharge to set it off. But, in contrast with the sound of thunder, the size of each disturbance radiated by electromechanical relaxation puts its spectral peak in the infrasonic portion of the spectrum. As Lamb showed, the length of the pulse radiated from a sphere under pressure is equal to the sphere's diameter. The dominant wave period contained in the N-shaped impulse is thus 2 a/C. In the case of a sphere of 5-km radius, the acoustic pulse length would be about 30 s, precisely in the spectral region of the observed waves. If the observed infrasound is composed of the superposition of such N-waves, somewhat smoothed and dispersed by various propagation effects (e.g., selective absorption, ducting), then we would expect pressure fluctuations with rapidly changing amplitude and spectral content, arriving from quickly changing directions. A

difficulty arises, however, with emission rates greater than about once every ten seconds, because the spectral content of the emissions would then reflect the repetition rate instead of the wavelength determined by the source size.

5.2.4 Objections to the Mechanism

The most serious objection to be raised against the electrostatic mechanism concerns the pressure waveform observed from nearby storms (see Figure 4). At such distances, propagation effects have negligible influence on the emitted waveform, which should be received virtually intact and should reveal the impulsiveness and intermittency that the electrical mechanism predicts. In fact, infrasound from nearby storms reveals no such effects (see also Bowman and Bedard, 1971).

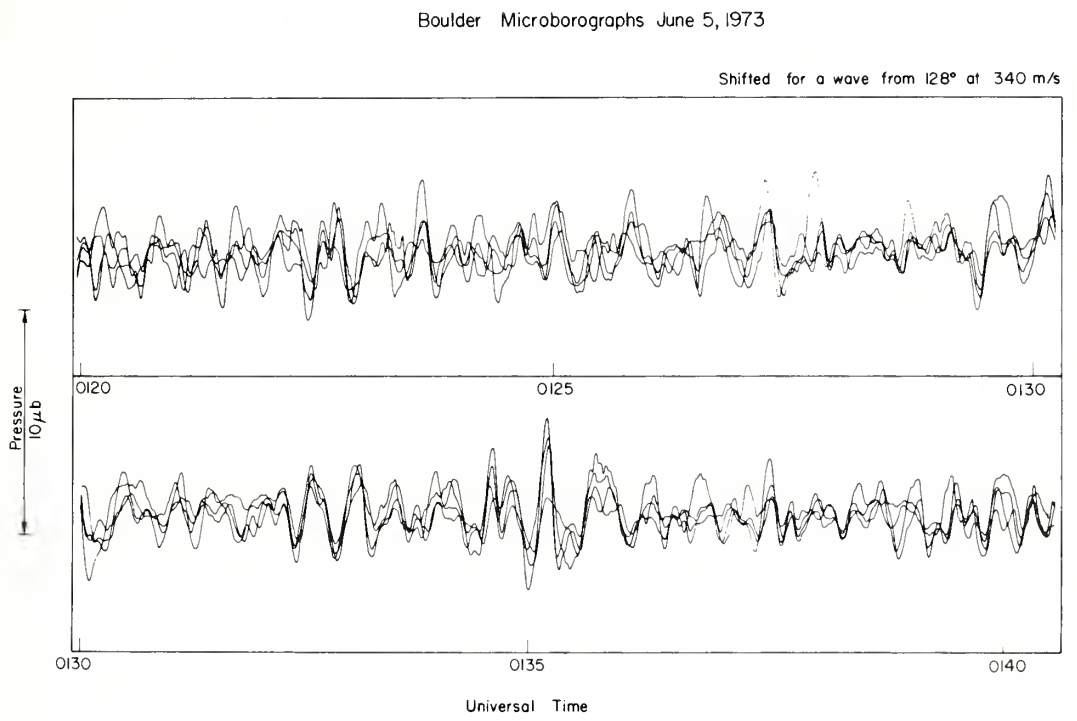

Figure 4a. Four superimposed microbarograph traces recorded at Boulder, Colo., during a severe-weather outbreak (including tornadoes) in Oklahoma during 1973. The four traces have been shifted in time for maximum cross-correlation; the shifts correspond to delays appropriate to a plane acoustic wave passing over the sensor array at 340 m/s from 128 deg azimuth. This acoustic event was monitored at Boulder for over 5 hours and was detected at six other observatories as far away as College, Alaska.

Another objection can be raised on the observational grounds that infrasound and electrical activity are not observed to be closely related. If the infrasound radiation mechanism were fundamentally electrical, we would expect at least two kinds of observational verification: First, there should be some statistical relation between the geographic and temporal distributions of infrasound sources and lightning activity. No such associations are evident. For example, a statistical maximum in lightning activity exists in Florida, yet no significant long-distance infrasound has been associated with Florida storms. (Some ionospheric infrasound has recently been observed in Florida by Prasad et al. (1975), however.)

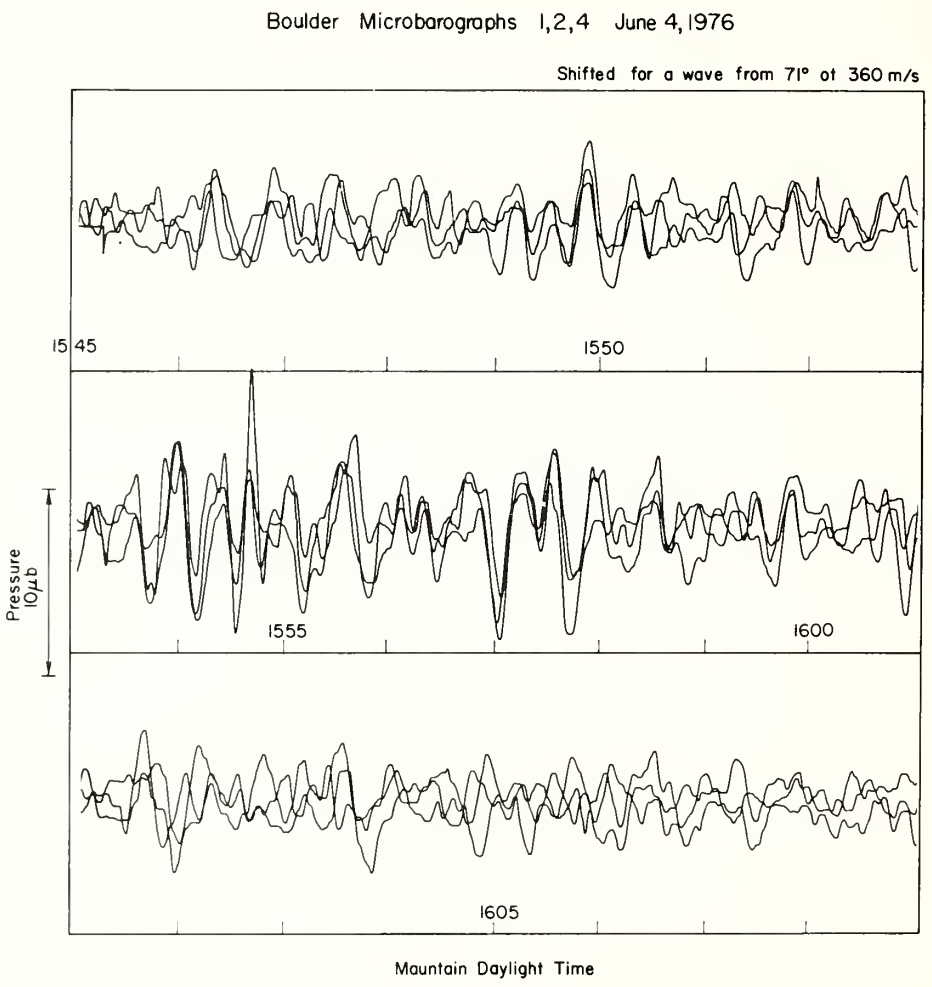

Figure 4b. Three superimposed microbaragraph traces recorded at Boulder, Colo., during the passage of a tornado about 27 km NE of the observatory. The traces have been shifted in time corresponding to a plane acoustic wave from 71 deg azimuth at 360 m/s, which coincides with the direction of the tornadic storm. Compare the characteristics of the waveform and its spectral content with the longer range event of Fig.4a.

Second, observable radio-frequency electromagnetic radiation should accompany individual infrasound radiation events. An experiment to observe such a connection has recently been carried out, and its results are reported in another paper (Beasley et al., 1976), but it will suffice to say here that no evidence of a connection has been found.

In summary, some features of the electrostatic emission mechanism seem to satisfy observational requirements; yet others remain unexplained. Because explanations can be conceived for the failures, I resist discarding this mechanism completely, and label it only "unlikely."

5.3 Nonlinear Pulse-Stretching

I examine one more process by which lightning discharges could be responsible for severe storm infrasound -- the possibility that nonlinear pulse stretching in the upper atmosphere shifts the energy in the lightning shock to the infrasonic portion of the frequency spectrum, where it can propagate to great distances relatively unattenuated.

This would work as follows: Some of the acoustic energy radiated as thunder reaches the upper atmosphere (100 to 120 km) before returning to earth (Figure 5). In propagating to such altitudes, the weak shock experiences $e^{z/2H}$ amplitude growth until propagation becomes nonlinear; the positive phase of the shock waveform travels faster than the lagging negative phase, and the pulse becomes stretched. When the pulse is refracted back to earth, its amplitude is diminished again, but its length remains stretched so that its spectral content is shifted to lower frequencies (see Figure 6).

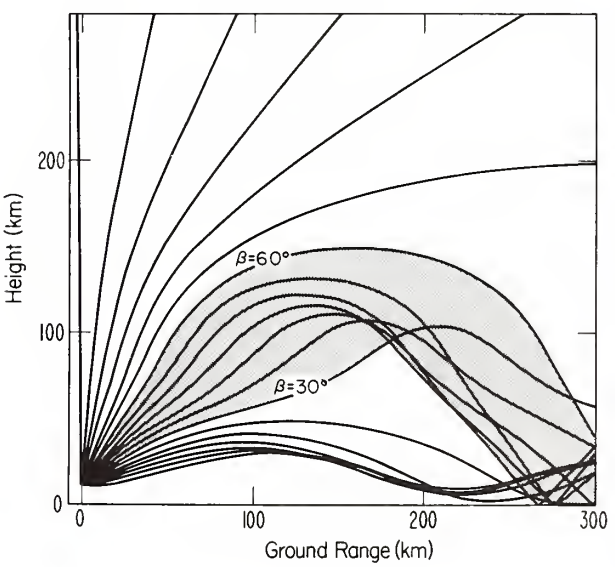

Figure 5. Acoustic raypaths in a realistic temperature profile with no winds. The source is at 10 km height, and rays are spaced 5 deg in elevation angle. The shaded region shows rays that reflect in the 100 to 150 km height range, and that could experience nonlinear pulse-stretching.

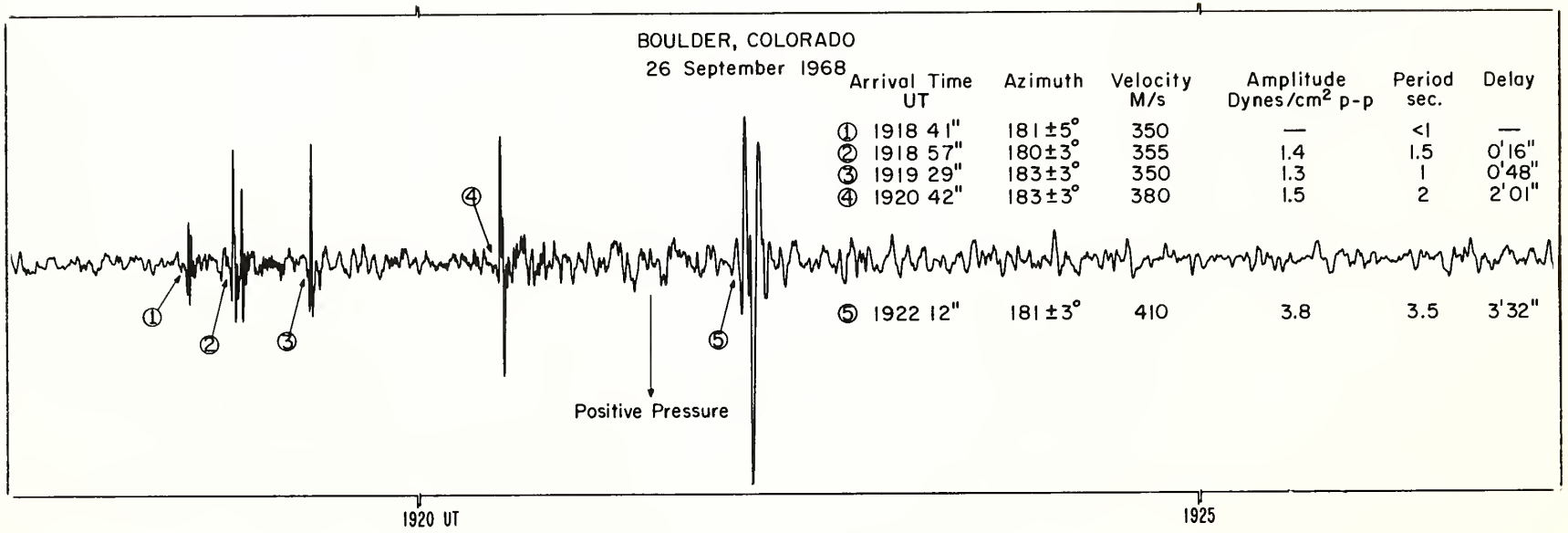

Figure 6. A microbarograph trace showing the sequential arrival of acoustic impulses at Boulder, Colo., probably from a distant supersonic aircraft. The time delays, and the increasing period and horizontal phase velocity of each successive arrival suggest that the latest arrivals traveled via the thermosphere and experienced nonlinear pulse-stretching. The amplitude increases may be caused by focusing.

5.3.1 Pulse-Lengthening Estimate

Daniels (1969) has adapted a formula of Reed's (1959) to calculate the amount of pulse stretching suffered by upward-traveling shock waves from explosions and from supersonic aircraft (sonic booms). Both our everyday experience and some measurements reveal that the fractional overpressures (at comparable distances) are about the same for thunder and for sonic booms (Daniels, 1969; Jones et al., 1968). Daniels gives a fractional overpressure of 2.36×10^{-4} at a reference distance of 17.1 km for a small supersonic-fighter aircraft and 5.6×10^{-4} for a larger aircraft (SST). Extrapolating the curves of Jones et al. (their Figure 1) to the same reference range shows that the range of values given for sonic boom overpressure corresponds to "typical" lightning flashes of 2 to 30 x 10^5 J km^{-1}. Their spectral contents (derived from the length of the positive pressure phase of the pulse) are also comparable. Therefore, within the accuracy of our knowledge of both phenomena, the pulse-stretching calculations Daniels did should apply to lightning shocks as well. He calculated pulse-lengthening factors of 13 to 17 times for waves reflecting at 110 km; the peaks of the frequency spectra were shifted to 0.4 and 0.13 Hz, well into the frequency range of interest to us. Multiple reflections between the ground and thermosphere could cause further lengthening (Figure 6).

5.3.2 Absorption Estimate

To find out if waves traveling such a path could actually be observed, we must also estimate the acoustic absorption suffered.

Lacking adequate theoretical or experimental information about nonclassical absorption mechanisms (e.g., by turbulence or molecular relaxation) at infrasonic frequencies, we estimate absorption caused only by viscous damping. The results should serve as a lower bound on the total absorption from all mechanisms. Several sources (cf. Reed, 1972; Procunier and Sharp, 1971) give the classical sound amplitude absorption coefficient α in the form

$$\alpha = kf^2/p \ , \tag{5.9}$$

where f is the wave frequency, and p is the ambient atmospheric pressure; k is a constant whose mean value in mks units is about 2×10^{-6}. The plane-wave acoustic amplitude is then calculated from

$$A = A_o \exp (Z/2H) \exp - \int_S \alpha \, ds, \tag{5.10}$$

over the path S, where H is the pressure scale height. The path S begins near the ground and terminates at a height Z. Formula (5.10) accounts for the competing effects of exponential amplitude growth and viscous attenuation, but ignores spherical divergence, which is of secondary importance.

Acoustic ray-tracing calculations (Figure 3) show that if acoustic rays are launched from 10 km altitude, rays having elevation angles β (from horizontal) between about 30 and 60 deg travel to heights between about 100 and 120 km before returning to the ground. These are the rays that could conceivably experience pulse-lengthening effects. We assume $\beta = 45°$ in the following estimates.

For heights to 130 km or so, we can assume that pressure p follows an exponential law of the form

$$p(z) = p(o)\ e^{-z/H}, \tag{5.11}$$

where z is the height and H is the pressure scale height, given a constant value 6.65 km here; p(o) is 10^5 N m^{-2}. We simplify our absorption estimate by assuming that the rays travel in straight-line triangular paths, reflecting at a height Z. The elevation angle β is then

$$\beta = \tan^{-1}\ (2\ n\ Z/D)\ , \tag{5.12}$$

where D is the total ground range and n is the number of ray "hops" between the ground and the thermosphere base. Substituting (5.9) and (5.11) into (5.10), we get the up-leg attenuation

$$\ln \frac{A}{A_o} = Z/2H - \frac{kf^2}{p(o)} \int_s e^{z/H}\ ds. \tag{5.13}$$

Substituting $dz = ds \sin\beta$ and integrating from z = 0 to Z, we get

$$\ln \frac{A}{A_o} = Z/2H - \frac{kf^2 H}{p(o)\ \sin\beta}\ (e^{Z/H}-1)\ . \tag{5.14}$$

The competing effects of exponential growth and viscous damping cause the wave to reach a maximum amplitude at the height where the growth rate equals the damping rate. This height increases with decreasing wave frequency. By differentiating (5.14) with respect to z we find Z_{max}, the height of maximum amplitude:

$$Z_{max} = H\ \ln \frac{p(o)\ \sin\beta}{2H\ k\ f^2}\ . \tag{5.15}$$

Table 5.1 gives values of Z_{max} for some frequencies of interest.

Table 5.1 Z_{max} Values

f(Hz)	Height of Maximum Amplitude (km)
0.1	128
1.0	98
10.0	67
100.0	37

These heights also happen to be very nearly the heights where damping alone reduces the wave energy by 3 dB:

$$Z_{3dB} = (96 - 13.3\ \ln f)\ \text{km}, \tag{5.16}$$

where f is in Hz. In general, the integrated ground-to-upper-atmosphere attenuation (in decibels) caused by viscosity alone is

$$\alpha = 1.63 \times 10^{-6}\ f^2\ e^{z/H}\ \text{dB}, \tag{5.17}$$

valid up to heights of about 130 km.

Taking z = 100 km,

$$\alpha = 5.54\ f^2\ \text{dB}, \tag{5.18}$$

giving about 11 dB attenuation per hop at 1 Hz, only 0.11 dB per hop at 0.1 Hz, but over 1100 dB per hop at 10 Hz. (The effects of exponential amplitude growth on wave amplitude cancel out on the up and down legs of each hop.)

Given a maximum stretching factor of about 20 and the excessive absorption of higher frequencies, the emitted waves must be at 1 Hz or lower frequencies, if thunder is to explain the infrasonic observations at 10 to 40 s wave periods. Yet measurements of thunder spectra reveal very little energy below 1 Hz.

5.3.3 Summary of Further Objections to the Mechanism

A. The lightning source is impulsive in nature and would require frequent and repeated strokes for several hours to account for the continuous waves that are observed.

B. Severe-weather infrasound is seen at distances from the apparent source storms that are too short (less than 300 km) to permit thermospheric reflection.

C. The ionospheric effects have periods of 2 to 5 min and persist for hours. The surface and ionospheric effects have such similar phenomenologies that a common source mechanism is suspected. Pulse stretching could not explain the low frequencies and continuous nature of the ionospheric effects.

6. VORTEX SOUND

As noted earlier, steady, subsonic flows (including steady vortices) emit no sound. But in the atmosphere, all organized vortex motion appears to be unsteady in some sense. All vortices are unsteady during their formation and their decay, and although the two processes are conceptually distinct, they probably overlap during the lifetimes of most atmospheric vortices. Furthermore, the flow inside what may appear to be a steady vortex often reveals smaller scale undulations or vortices, or it may contain fully developed turbulence. These observations are consistent with many theoretical analyses (cf. Lord Kelvin, 1910), which demonstrate that vortex flow is unstable with respect to many kinds of radial and axial perturbations. Therefore, we would expect most atmospheric vortices to radiate acoustic energy; furthermore, we would expect their rotation and cylindrical geometry to favor the sustained generation of particular wave frequencies.

There is ample evidence, based mostly on observations of motions on scales that produce audible sounds, that vortices do radiate. The aeolian tone (cf. Powell, 1964; Richardson, 1924) is the classical example. There, vortices that form in the wake of a cylindrical obstacle placed in an airflow are shed at a characteristic rate and generate sound at the shedding frequency. Some musical instruments are based on a phenomenon known as the "edge tone" (Powell, 1961), in which sound is radiated by the vortex pairs that form periodically when an airstream impinges on a wedge-shaped obstacle. Chanaud (1969) studied the aerodynamic sound radiated by a rotating disk in air and found that periodic vortex motion around the disk's periphery was responsible for some of the lowest-frequency radiated sound. The same sort of peripheral turbulence (or perhaps more orderly peripheral vortices) could explain reports of "musical sounds" emitted by tornadoes (Abdullah, 1966). Dynamically similar motions, but on larger scales, could radiate infrasound that would go mostly unobserved. I now examine how mesoscale vortices form and dissipate in the atmosphere, with specific attention to those associated with convective storms. Then I estimate how much radiation could be expected from two simple examples of unsteady vortex flow.

6.1 Vortex Formation

Apart from mesoscale vortices that are mechanically produced, for example, in the flow past mountains and islands (Chopra, 1973, and references therein), atmospheric vortices all involve the coupling of ambient vorticity with strong buoyant convection (Morton, 1966). But convection-associated horizontal convergence, operating on the background vorticity due to the earth's rotation alone, is insufficient to explain the observed intensity and development times of the mesoscale vortices, especially tornadoes, associated with thunderstorms. Such vortices must form as a result of vigorous convection in a neighborhood with a richer distribution of vorticity than that due to the earth's rotation alone (about 10^{-4} s^{-1} at midlatitudes). In the case of squall-line thunderstorms, additional background vorticity is available from the synoptic situation. In the vicinity of a front, strong cyclonic circulation is often present on a synoptic scale, and can contribute about an additional 10^{-4} s^{-1} vorticity. Furthermore, frontal systems are likely to be rich in the potential vorticity that arises whenever the constant-density surfaces are inclined to the constant-pressure surfaces (producing solenoids).

The horizontal vorticity associated with vertical wind shear in the boundary layer is generally around 10^{-2} s^{-1}. Convection can draw up and stretch loops of formerly horizontal vortex tubes (the so-called "tilting term" in the vorticity-tendency equation), causing an intensified, erect vortex pair with opposite rotation senses (Davies-Jones and Kessler, 1974). Such pairs are now commonly seen inside storms with Doppler radars (cf. Kropfli and Miller, 1976). Similar vortex-pair formation has been observed by Idso (1975) in the airflow over hills.

Another kind of unsteady vortex flow is favored during strong convection when certain relationships between the horizontal inflow angle and the "configuration ratio" are satisfied. (The configuration ratio, or aspect ratio, is the ratio of the diameter of the zone of convection to the height of the inflow layer.) In laboratory simulations of tornado-like vortices, Ward (1972) demonstrated conditions that favor the production of multiple vortices rather than a single one:

> "In the laboratory, more than one vortex can be produced only when the configuration ratio is greater than unity. When the ratio is 4, and the angle of inflow (measured from a radial) θ is very small, 2 to 3 deg, a single vortex forms; as θ is increased, the diameter of the core increases proportionately. The scale of the turbulence also increases with the inflow angle, and when the latter reaches about 30 deg, a vortex pair develops. They are located on opposite sides of the parent vortex near the radius of maximum tangential speed, and the pair rotates around the central axis at about half that speed. Once the pair is formed, the flow becomes somewhat more stable, and the cores are well defined. This mode will continue when the inflow angle is decreased several degrees below that required for pair formation.

After a pair is formed, a third vortex will form, and then a fourth, as the inflow angle is further increased. In general, the greater the number of vortices in the system, the smaller their individual core diameters.

The critical inflow angle, θ_c, at which multiple vortices form is very sensitive to the geometry of the convection. A vortex pair forms at an inflow angle of about 30 deg when the configuration ratio is 4; when that ratio approches unity, the angle required for pair formation increases to about 75 deg. When the depth of the convergence layer exceeds the diameter of the convection, no multiple vortices have been observed."

Davies-Jones (1973) reinterprets Ward's results, stating that the experimental transition from a single wide vortex to a pair of concentrated vortices occurs at a critical "swirl ratio," rather than a critical inflow angle. The swirl ratio is the ratio of maximum tangential speed to the mean updraft speed. Evidently, a system of multiple corotating vortices often represents a stable configuration under some ambient conditions in which a single vortex would be unstable. Next, we find that similar multivortex systems can form during the breakdown of a single steady vortex.

6.2 Vortex Breakdown and Dissipation

A simple calculation shows that storm-scale atmospheric vortices (including tornadoes) would have lifetimes of more than a year if molecular viscosity were the sole dissipating agent. To get decay times compatible with those observed (tens of minutes), we need viscosity coefficients about 10^5 greater than reasonable values for the molecular viscosity of air; that is, about 1 to 10 $m^2\ s^{-1}$ is required. If we attribute this damping process to eddy viscosity, we can estimate the eddy size ℓ_e required by ν_e/u_e, where ν_e is the eddy-viscosity coefficient and u_e is a typical eddy-associated air velocity. For realistic velocities, we get an eddy size of a few meters. We can thus picture a vortex surrounded by a mixing region, perhaps a few meters thick, through which momentum is transmitted to the environment by eddies of various sizes.

There is now substantial evidence that, in many cases, the early stages of vortex breakdown and dissipation are characterized not by a broad spectrum of eddy sizes, or "turbulence," but rather by oscillatory and quasi-periodic motions resulting from various kinds of vortex instability (Lord Kelvin, 1910). In fact, several kinds of observations suggest that certain peripheral wave numbers are preferred and that vortex breakdown into a small number of well-defined smaller vortices may be common in the atmosphere.

Fujita (1970, 1971) has shown evidence for the existence of "suction vortices" around the peripheries of tornadoes and dust devils. These suction vortices appear as a ring of smaller, intense vortices that rotate about the axis of a weaker parent vortex. Weske and Rankin (1963) demonstrated in the

laboratory the existence of well-defined periodic vortices spaced around the periphery of a rotating disk in water. (A solid, rotating disk can be thought of as representing the viscous core of a parent vortex.) These vortices seem to be the cylindrical analogs of the boundary-layer eddies that form in the flow over a plane, rough surface, but with the additional requirement of an integer number of eddies around the disk's periphery.

The fact that many tornadoes leave sequential ground tracks resembling cycloidal orbits is interpreted as strong evidence that many tornadoes are actually sub-vortices orbiting inside larger-scale "tornado cyclones" (Agee et al., 1976). Earlier, Darkow (1971) had presented a statistical analysis of the periodicity of tornado production in selected tornado "families", which suggested a mean interval of 45 min between successive tornado touchdowns.

A detailed case study of a multifunnel tornado by Agee et al. (1975) revealed a parent tornado vortex with a 300 m diameter, around which rotated as many as seven secondary vortices, some of which became tornadoes. These peripheral vortices were observed to grow or dissipate, depending on which side of the parent vortex they were on (with respect to the direction they travel as a whole), and they had 30- to 60-m diameters. The tangential velocity of the subsidiary vortices about a common center varied with position in the parent vortex and ranged between 25 and 55 m s^{-1}, corresponding to ground speeds of up to 75 m s^{-1}. The secondary vortices thus tend to bunch up near the trailing edge of the parent vortex.

We estimated a frequency associated with the secondary-vortex motion by examining Figure 14 of Agee et al. (1975) and estimating the times between the appearance of successive vortices at the same location along the periphery of the parent. Three time intervals between the passage of successive vortices past the 9 o'clock position on the parent were 10.3, 8.7, and 3.2 s. If acoustic waves were radiated from the system, the spectrum of the radiation would be in the same period range (see Sec. 6.3.1). Unfortunately, no microbarographs were suitably placed to detect any such radiation from this storm.

A picture is now emerging (Agee et al., 1976) of a complex hierarchy of vortices and sub-vortices associated with some tornadic storms. The hierarchy extends through: (a) the "tornado cyclone", perhaps 5 km in diameter, which probably coincides with "hook echoes", as well as cyclonic features observed with Doppler radars and may be exhibited visually in the "wall" or "pedestal" clouds often accompanying tornadoes; (b) a "mini-tornado-cyclone", perhaps several hundred meters in diameter, corresponding to the "parent" of multiple tornadoes; (c) tornadoes themselves, up to a few tens of meters in diameter; to (d) the sub-tornado-scale "suction vortices", up to a few meters in diameter, proposed by Fujita, which are probably responsible for the most intense damage. Figure 7 illustrates such a vortex hierarchy.

Such a picture suggests the importance of the role played by dynamic instabilities, as opposed to turbulence, in the decay of thunderstorm vortices. Theoretically, instabilities in cylindrical flows can take many forms, from a simple two-dimensional roll-up to complex three-dimensional (e.g., helical)

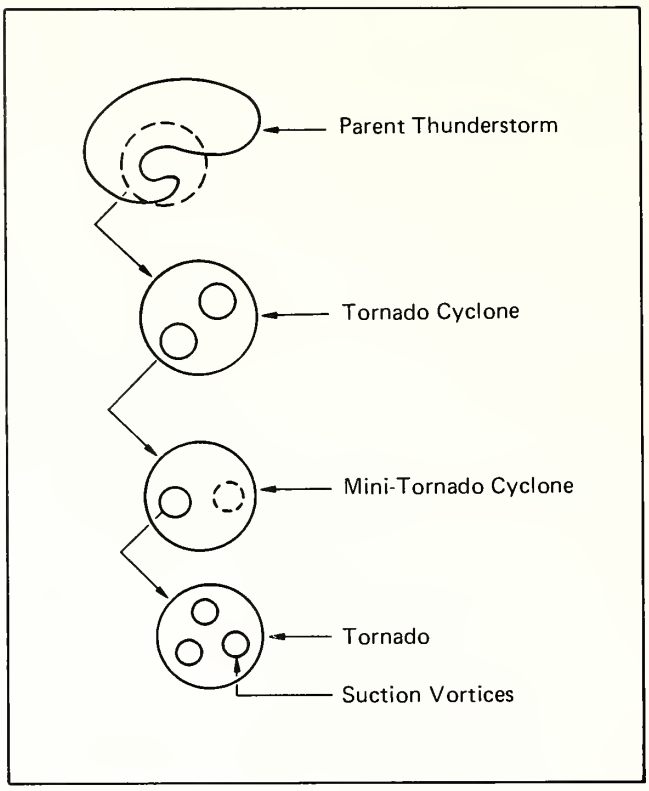

Figure 7. A schematic of a possible hierarchy of multiple-vortex systems for the various scales of motion associated with a tornado-producing thunderstorm (after Agee et al., 1976).

structures (cf. Davy et al., 1968). For example, a vortex is unstable with respect to radial perturbations if, within some annulus, angular momentum decreases with increasing radius from the axis of rotation (Rayleigh's criterion) (Yih, 1969; Chandrasekhar, 1961). Other instabilities resemble the Kelvin-Helmholtz instabilities in plane-stratified shear flow, with centrifugal force playing the role of gravity. The number and sizes of the smaller vortices into which a larger vortex breaks down are governed by the intensity and thickness of a high-shear annulus and its circumference.

The same laboratory simulations of tornado-like vortices cited earlier (Ward, 1972) have verified that vortex breakdown can be accompanied by the formation of a few vortices of next-smaller scale:

> "In the experimental apparatus, when (the convection diameter) approaches a critically large value, a single vortex becomes unstable, with accompanying large scale turbulence and large fluctuations in core diameter. It appears that this

instability is the result of the presence of inward directed forces associated with radial (inward) momentum flux sufficient to produce a vortex core whose central pressure deficit requirement is greater than can be maintained in the presence of subsidence in the large core. In this condition of instability, when one or more vortices of smaller horizontal scale form in the annulus of [Figure 8], they tend to be stable, since their smaller cores can maintain a greater pressure deficit".

For our purposes, it is not so important to understand the details of the instabilities that may cause vortex breakdown as it is to recognize that the breakdown process can often be described in terms of relatively orderly and long-lived subsidiary flows.

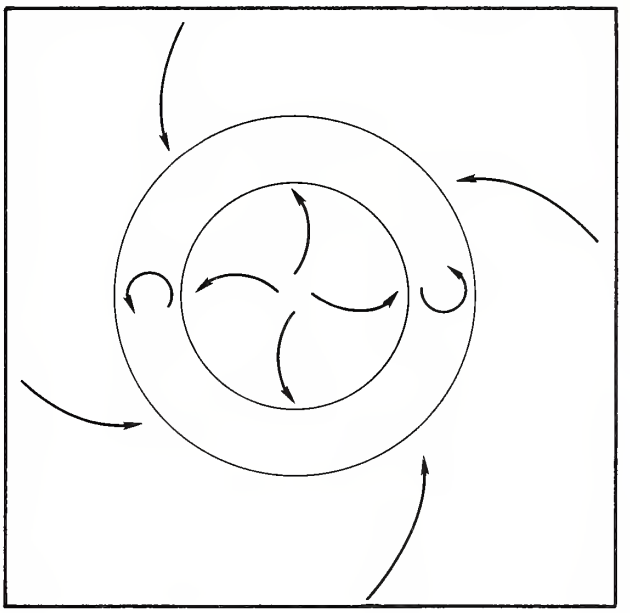

Figure 8. A sketch of the surface flow pattern observed by Ward in laboratory modeling of vortex-pair generation.

6.3 Acoustic Radiation by Unsteady Vorticity

Powell (1964) developed a "theory of vortex sound," in which the sound radiation from a low-speed compressible flow can be estimated when only the spatial and temporal distribution of vorticity is known. This was an important advance from our point of view; we can now compute the acoustic field in terms of observables that do not involve the fluid's compressibility or other difficult-to-estimate quantities like the distribution of Reynolds stresses in the fluid. Some features of the airflow in and around storms (such as those just discussed) lend themselves to description in terms of simple vorticity distributions.

Powell's general expression for the far-field acoustic velocity perturbation $\underset{\sim}{u}(\underset{\sim}{x})$ at a distant observation point $\underset{\sim}{x}$ is

$$\underset{\sim}{u}(\underset{\sim}{x}) = - \frac{\hat{x}}{4\pi x C^3} \int_{V_o} y_x \, L_x'' \, dV(\underset{\sim}{y})^* \, . \qquad (6.1)$$

The quantity L_x'' is the x component of the second time derivative of ζ x u, where ζ is the vorticity and u is the velocity field in the source volume V_o; y_x is the x component of the spatial source-integration variably y; $\hat{x}$ is a unit vector in the x direction, and the asterisk indicates the usual time retardation, the only effect of the fluid's compressibility explicitly considered. This approach becomes intuitively palatable if the analogy with electromagnetic fields is considered: if ζ represents an electric current distribution, then $\underset{\sim}{u}$ represents its magnetic field.

Powell applied his result to the radiation from a corotating vortex pair and to the aeolian-tone radiation by vortices shed from obstacles. I apply his results to storm-scale airflow and estimate the properties of the radiated infrasound.

6.3.1 Radiation From a Corotating Vortex Pair

When two or more vortices form near each other they interact, roughly speaking, as though each were a passive tracer in the velocity field of the other. A counterrotating vortex pair, for example, undergoes simple translation in a direction perpendicular to the plane containing their axes, and a corotating vortex pair rotates about a common axis in the same direction that each individual vortex rotates. The translating pair is of no direct interest acoustically, but the rotating pair does radiate.

The hydrodynamic velocity field of the corotating pair is qualitatively illustrated in the streamline pattern of Figure 9. It is apparent that, as this noncircular streamline pattern rotates, the external fluid experiences a radial force whose amplitude passes through two cycles for each single rotation of the vortex pair. Acoustically, then, the rotating streamlines produce the same effect on the external fluid as a rotating lateral quadrupole, as shown in Figure 9. Powell (1964) has calculated the acoustic radiated power, Π, starting with Eq (6.1), and using the following model.

In a fluid of density ρ and sound speed C, let two parallel line vortices of axial length ℓ, equal strength Γ and separated a distance 2r spin about an axis midway between them (Figure 10). The radiated power is,

$$\Pi = \frac{16}{15\pi} \frac{\rho}{C^5} \left(\frac{\Gamma}{4\pi r}\right)^8 \ell^2 . \qquad (6.2)$$

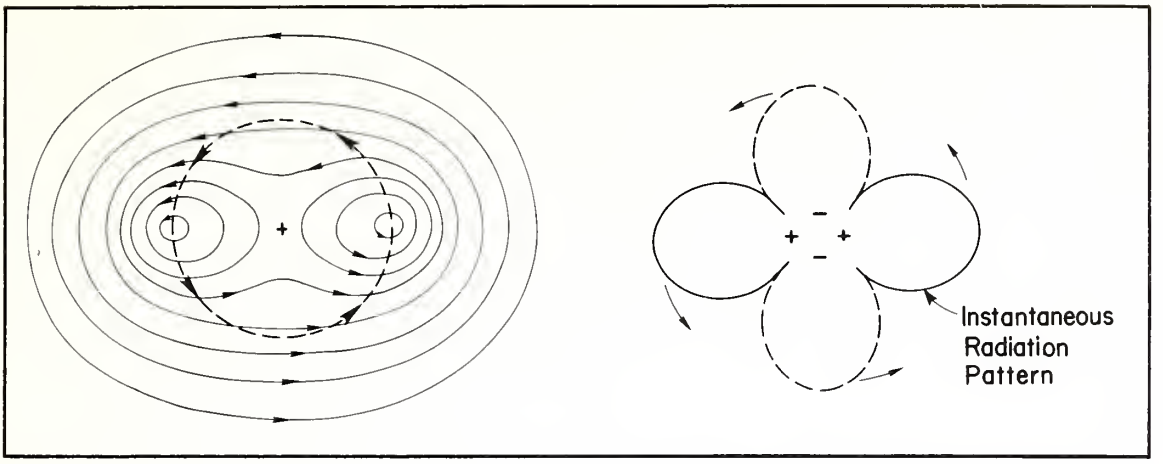

Figure 9. The streamline pattern calculated for a pair of corotating line vortices of equal strength (left), and the resulting instantaneous, rotating acoustic radiation pattern (right), which is equivalent to that of a rotating acoustic quadrupole.

The quantity $\Gamma/(4\pi r)$ is the velocity u at which the vortices spin about the common axis, and therefore their angular spin rate is $\omega = \Gamma/(4\pi r^2)$. Because the spinning vortices generate a hydrodynamic (and also acoustic) field like a fluid quadrupole, the radiated frequency is twice the rotation frequency: $f = \omega/\pi = \Gamma/4\pi^2 r^2 = u/\pi r$.

By comparing the power and frequency given by the spinning-vortex model with those associated with infrasound observations, we can estimate the required vortex parameters. First, we see that, independent of frequency,

$$u = \frac{\Pi^{1/8}}{K^{1/8} \rho^{1/4}} \quad , \tag{6.3}$$

where $K = \frac{16}{15\pi}$ and $\frac{\rho}{C^5} = 8.97 \times 10^{-14}$ for standard conditions (MKS units).

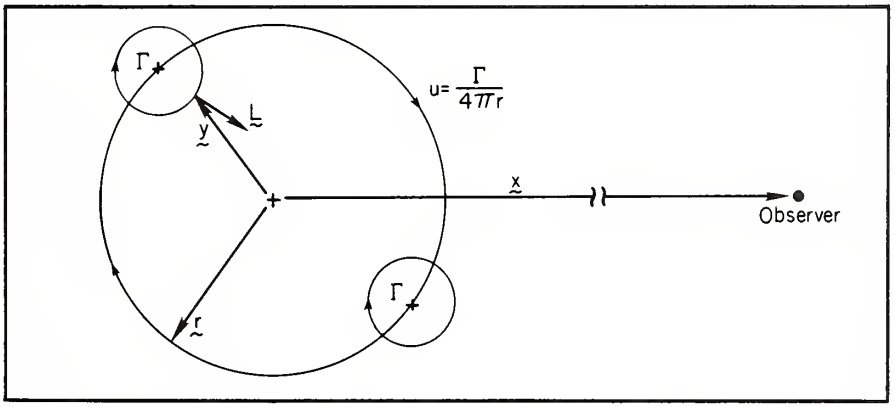

Figure 10. Geometry and notation for calculating the acoustic radiation from a corotating vortex-pair. Symbols are defined in the text.

Table 6.1 Required Vortex Corotation Speeds

Π(Watts)	ℓ=1 km u (m s^{-1})	ℓ=3 km u (m s^{-1})
10^7	57	43
10^8	76	57
10^9	101	76

Table 6.1 gives, for ℓ = 1 km and 3 km, values of u required to radiate 10^7, 10^8 and 10^9 W. Because this radiation mechanism is fundamentally monochromatic, we can compare these results with the 3 x 10^7 W source power estimated by Georges (1973) from both the ionospheric and surface pressure measurements. (The 10^8 to 10^9 W estimated source power we used, for example, in the turbulent source calculations, is an estimate of the total broadband radiated power.) A 3 x 10^7 W radiated power would require eddy spin speeds of about 50 m s^{-1}, a little high, but not in serious disagreement with motions observed in the most severe storms (Brown et al., 1971; Agee et al., 1975).

Since f = u/πr, we can calculate the value of r for the previously tabulated values of u and for two wave periods, 30 and 200 s (representing the observed wave periods on the ground and in the ionosphere). Table 6.2 shows values of r corresponding to the values of u given in Table 6.1.

Table 6.2 Required Vortex Separation

u (m s^{-1})	τ = 30 s r (km)	τ = 200 s r (km)
43	0.41	2.74
57	0.54	3.62
76	0.73	4.87
101	0.96	6.42

Thus, the surface observations require an eddy separation 2r of about a kilometer, and the ionospheric observations about 6 km. Eddies of the larger scale are now visible inside thunderstorms observed with dual-Doppler radars (Kropfli and Miller, 1975, 1976), but structural details of the eddies and their time variations are still beyond the resolution of current remote-sensing instruments. Counterrotating vortex pairs have been seen with Doppler radars inside some thunderstorms; they have diameters of up to 5 km and extend in height through most of the storm. The required spin rate for two vortices equals one half the acoustic radiated frequency, but would be correspondingly smaller for more than two vortices.

Using the circulation theorem, we can get a rough indication of the average vorticity corresponding to each case:

$$\zeta_{av} = \frac{2u}{r} \quad . \tag{6.4}$$

For example, for the case $u = 43$ m s^{-1} and $r = 2.74$ km, $\zeta_{av} = 0.03$ s^{-1}; for the case $u = 101$ m s^{-1} and $r = 0.96$ km, $\zeta_{av} = 0.21$ s^{-1}. For comparison, the vorticity in the core of a typical tornado has been estimated at about 1 s^{-1} (Davies-Jones and Kessler, 1974), and the maximum vorticity measured in a Colorado thunderstorm with Doppler radars is about 0.01 s^{-1} (Kropfli and Miller, 1976).

The radiated power depends only on the speed that the vortices spin around each other, but as the system becomes larger while keeping the radiated power constant, the angular spin rate, and thus the radiated frequency, is lowered. In other words, the wavelength of the radiation is related to the vortex-pair geometry by

$$\frac{\lambda}{\pi r} = \frac{C}{u} \quad . \tag{6.5}$$

Equation (6.1) tells us that, in a turbulent flow, where eddies of all sizes are present, the most powerful acoustic radiation tends to be from the largest eddies. Because of the separation factor y_x, it is the moment of vorticity that generates sound. In the case of thunderstorms, then, the motion of storm-scale eddies would cause the most intense radiation. This is consistent with the prediction of a turbulent description of the storm's motions.

The rotating-pair model is only one example of many kinds of unsteady vortex motion. Because vortex motion is unstable with respect to almost any kind of perturbation, a corresponding variety of possible acoustic-radiation mechanisms exists. Radial oscillations and helical instabilities could be modeled exactly and their radiation predicted, but we have no observations to indicate which model to choose. In any event, we would expect results quantitatively similar to those obtained with the corotating pair. Other

multiple-vortex systems can assume complicated rotating configurations, especially if many vortices of different strength and orientation interact. Their acoustic radiation would be correspondingly complicated, and a turbulent model would be required to represent all but the simplest configurations.

6.3.2 Aeolian-Tone Radiation

Assume that some part of a convective storm, probably the intense updraft core, forms an obstacle and diverts the middle-level wind flow. This assumption is supported by the observations by Fujita and Arnold (1963) and by Jessup (1972), who found blocking of the flow on the upwind side of storms and velocity maxima on their flanks.

Next assume that suitable conditions frequently exist for the generation and shedding of coherent vortices from the storm-obstacle, in a manner dynamically similar to the production of Karman vortex streets on a laboratory scale. This assumption can be justified on observational grounds from space observations of trailing vortices in the lee of islands, made visible by cloud patterns (cf. Chopra, 1973; Zimmerman, 1969, and the references they cite). The radar observations by Jessup (1972), and by those he cites, appear to show similar vortices in the lee of some thunderstorms.

The apparent dynamic similitude of mesoscale and laboratory-scale vortex streets requires some theoretical explanation. A well known condition for the formation of a train of discrete vortices behind an obstacle (usually a circular cylinder) in air or water on a laboratory scale is that the Reynolds number lie roughly in the range $10^2 < R_e < 10^5$. Here, the Reynolds number, $u\ell/\nu$, is defined in terms of the ambient flow velocity u, the diameter ℓ of the obstacle and the kinematic viscosity ν of the fluid. If the Reynolds number is lower than specified, the flow tends to be laminar; if larger, the flow in the wake of the obstacle tends to be fully turbulent. The periodic shedding of vortices represents the transition regime between a laminar and a turbulent wake. On a laboratory scale, the required Reynolds numbers are consistent with the kinematic molecular viscosities of the fluids used, but if one tries to explain the mesoscale eddies in the same way, kinematic viscosities result that are much too large to be attributable to molecular processes. Zimmerman (1969), Goldman and Wilkins (1973), and others have pointed out that the concept of eddy viscosity must be invoked if effective Reynolds numbers in the required range are to be obtained. Eddy viscosity arises in a turbulent "mixing region" between the environmental flow and internal storm circulation. Coefficients of eddy viscosity of the order of 10^2-10^3 m^2 sec^{-1} are required in the case of thunderstorm-obstacles.

In the theory of aeolian tones (cf. Powell, 1964, and the many references he cites) the vortex-shedding frequency (that is, the rate at which vortices are shed from one side of the obstacle) corresponds to the frequency of the emitted tone. Laboratory experiments have established empirically

that, within the required range of Reynolds numbers, the vortex-shedding frequency f_s is nearly proportional to the stream velocity U and inversely proportional to the obstacle diameter D (Figure 11). The constant of proportionality is called the Strouhal number S, so that

$$f_s = \frac{SU}{D} \quad . \tag{6.6}$$

Measured values of S are always in the neighborhood of 0.2, even when eddy viscosity plays a role (Goldman and Wilkins, 1973). We can thus estimate the U/D ratios that would be required to explain the observed infrasound wave periods τ. Using

$$D/U = \tau/5, \tag{6.7}$$

we get for τ = 20 s, U/D = 0.25, and for τ = 200 s, U/D = 0.025. If we let U be no larger than 50 m s^{-1}, then D must be smaller than 200 m (for τ = 20 s) or 2 km (for τ = 200 s). These obstacle sizes seem rather small in view of radar data, which suggest an obstacle size of 5 to 10 km. A 10 km diameter yields a 1000 s shedding period (for u = 50 m s^{-1}).

Using a formula given by Phillips (1956) for the intensity of aeolian tones, we get for the total radiated power

$$\Pi = 0.2\pi^2 \rho^2 l D U^6 S^2 / C^3, \tag{6.8}$$

where ρ is the atmospheric density and l is the obstacle length. Taking u = 50 m s^{-1}, l = D = 5 km, ρ = 1.2 kg m^{-3}, S = 0.2, and C = 340 m s^{-1}, we get $\Pi = 1.27 \times 10^9$ W. The power level is thus in the experimental range, but the wave period (about 8 min for the values used) is too long.

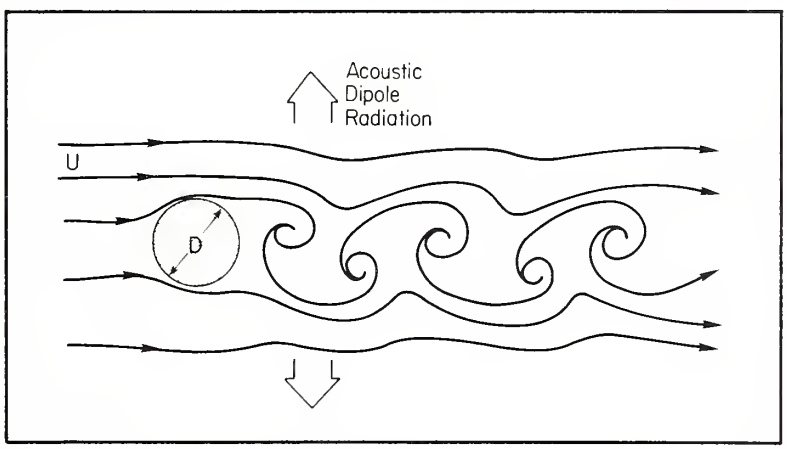

Figure 11. Sketch of the streamlines in the flow past a cylindrical obstacle under conditions that permit a train of wake vortices to be shed from the obstacle. Acoustic waves are emitted at the shedding frequency in a dipole-like pattern.

7. HEAT-DRIVEN OSCILLATIONS

It has been known for a long time that gas flows through systems containing a heat source can produce acoustic oscillations that are coupled with a periodic heat release by the heat source (Rijke, 1859; Rayleigh, 1878, 1879; Merk, 1956; Mawardi, 1956). Such oscillations are called heat-driven oscillations. In general, coupling between a flow and a heat source occurs when fluctuations in the flow parameters (pressure or temperature, for example) influence the rate of heat release, and when, in turn, fluctuations in heat release influence the flow state variables. Instability and oscillations occur when the heat source reacts to perturbations in the proper phase to reinforce the perturbations. The initial fluid fluctuations may be either small-amplitude acoustic waves or random fluctuations carried by the flow. Oscillations at particular frequencies are often enhanced by direct acoustic feedback, as when the system is enclosed in an acoustic resonator. Such oscillations are observed in certain kinds of "singing flames," and sometimes have destructive effects in industrial combustion systems and in jet and rocket engine combustion chambers (see the review paper by Putnam and Dennis, 1956).

The question I ask here is whether similar oscillations, and the associated sound radiation, could be caused by the interaction between a convective storm's updraft and the release of the latent heat of vaporization where water droplets condense. One could qualitatively argue as follows:

Suppose initial fluctuations in (say) temperature pass through the saturated air inside a storm, either in the form of small-amplitude acoustic waves or as fluctuations in the updraft current. An air-temperature increase should quickly heat up the water droplets and cause an increase in evaporation (assuming buoyancy effects occur much more slowly). As the droplets evaporate, they cool and draw heat from the surrounding air, thus cooling it by conduction. But this process takes time: There are characteristic time scales associated with the transfer of mass, heat and momentum among the water droplets, the dry air and the water vapor components of the mixture. If the air temperature responds to the droplet cooling just as a negative temperature phase of the initial fluctuation passes through the region, then that frequency component of the fluctuations should be reinforced. During the negative temperature cycle, increased condensation would be encouraged, releasing more latent heat, which heats up the surrounding air in time for the arrival of the next positive temperature phase of the initial fluctuation. Thus, the frequency component of the temperature fluctuations that coincides with the time scale of latent heat transfer would be amplifed, would extract energy from the heat source, and would radiate it away as sound.

This qualitative argument can be submitted to quantitative examination by analyzing the propagation of plane acoustic (or acoustic-gravity) waves in an infinite, saturated environment, as has been done, for example, by Einaudi and Lalas (1973) and by the earlier workers they cite. Their results show that, for waves with very long, gravity-wave periods, the effect of condensation is essentially to change the effective Brunt-Väisälä frequency in the wave-dispersion relation. At these low frequencies, the water droplet mass,

velocity, and temperature respond fully to environmental (i.e., wave-associated) changes and remain nearly in equilibrium with the air. For audible acoustic waves, on the other hand, the condensation time constants are much longer than a wave cycle, so that the condensation process just barely gets started before the wave cycle reverses. The net effect of the resulting lag is a relaxation type of absorption in saturated air. The frequency range that interests us lies between these two extremes, when a wave period may be comparable with the time scale of the phase-exchange process.

The problem of sound propagation in a condensing vapor has been analyzed by Marble and Wooten (1970), Marble (1969), Cole and Dobbins (1970), Einaudi and Lalas (1973), and others. The analysis by Marble and Wooten appears to apply at any wave frequency and is most readily applied to a quantitative treatment of our problem. They have obtained wavelike solutions of the six equations representing continuity, motion, and energy for the gas phase, motion and energy of the liquid (droplet) phase, and a vapor phase equation of continuity. They have obtained a general acoustic-wave dispersion relation of the form

$$\frac{CK^2}{\omega} = \frac{(Z_1-i\omega)\quad(Z_2-i\omega)\quad(Z_3-i\omega)}{(\Omega_1-i\omega)\quad(\Omega_2-i\omega)\quad(\Omega_3-i\omega)}\ , \tag{7.1}$$

which applies over all frequency ranges. The parameters Z_i and ω_i are complicated functions of the vapor and droplet mass fractions, the specific heat ratio and the latent heat of vaporization; $K = K_1+iK_2$, the complex wave number. From (7.1) we obtain the imaginary part of the wave number, i.e., the attenuation coefficient:

$$\frac{2CK_2}{\omega} = \frac{\omega(Z_1/\Omega_1-1)\cdot\omega(Z_2/\Omega_2 1)\cdot\omega(Z_3/\Omega_3-1)}{(1+\omega^2/\Omega_1{}^2)\cdot(1+\omega^2/\Omega_2{}^2)\cdot(1+\omega^2/\Omega_3{}^2)}\ , \tag{7.2}$$

assuming $\frac{CK_1}{\omega} \simeq 1$. If amplification were possible, the attenuation coefficient would go negative for some realistic values of the system parameters. However, the quantities Z_i/Ω_i are always greater than unity. Thus the wave is always attenuated, and the attenuation coefficient exhibits maxima at wave frequencies corresponding to $\omega=\Omega_i$, which are characteristic frequencies related to the mass, momentum, and heat-transfer times of the system.

For wave frequencies much smaller than the frequencies corresponding to the usual thermal and viscous time constants in the system (i.e., about 100 Hz) Marble and Wooten get an attenuation coefficient α

$$\frac{\alpha}{\omega} \simeq \frac{\gamma}{2} K_V(\eta-1)^2 \frac{\omega\tau_D/K_P}{1+(\omega\tau_D/K_P)^2}\ , \tag{7.3}$$

where ω is the acoustic wave frequency, γ is the specific heat ratio and K_v and K_p are the mass fractions of water vapor and water droplets (assumed small); η is the latent heat parameter L/C_pT, where L is the latent heat of vaporization, and C_p is the specific heat at constant pressure of the gas and T is its temperature; τ_D is the mass-diffusion time associated with droplet evaporation. Thus, attenuation at these frequencies always increases with the vapor mass fraction and the latent heat parameter. Attenuation reaches a maximum at a frequency $\omega = K_p/\tau_D$, which, for typical cloud parameters, is about a 1-s wave period.

To reconcile this result with the qualitative argument at the beginning of this section, it is useful to examine the transient solutions obtained by Marble and Wooten, which reveal the response of the system variables to a step discontinuity in air pressure and temperature. The water droplets respond in two phases to an initial step increase in air temperature: First the droplets are exponentially warmed by conduction from the air on a time scale of about 0.01 s, with relatively little change in air temperature. Evaporation begins when the saturation vapor pressure near each droplet surface has been raised above the ambient vapor pressure. It takes about 0.01 s for evaporation to begin after an initial air temperature rise. Evaporation cools the droplets and the newly evaporated vapor, and the gas is eventually cooled exponentially by conduction on a time scale of about 1 s. The final equilibrium gas temperature is determined by the amount of liquid present and the latent heat of vaporization. The net effect is that droplet evaporation absorbs heat from the gas whenever the temperature perturbation is positive; conversely, condensation at the droplet surface releases heat whenever the temperature perturbation is negative. Whatever the sign of the air temperature perturbation, the heat source acts to oppose it. Thus, the heat source responds to a sinusoidal temperature perturbation whose frequency corresponds to the evaporation time scale (about 1 s), by opposing the excitation with a slight time lag. The net result is absorption of the perturbing wave, and not reinforcement. Thus, the mechanism is not a viable source process.

7.1 Condensation in a Supersaturated Environment

Another acoustic source mechanism has been suggested that is related to the heat-driven oscillations just examined. If condensation commences in a supersaturated region of the atmosphere, the condensation boundary should move outward with a speed limited by the sound speed. Corresponding density changes should move with the boundary, and an acoustic impulse should be radiated. Rapidly building towers in some cumulonimbi may be visual manifestations of such moving condensation boundaries.

It is difficult to construct a realistic quantitative model of this process from which the acoustic radiation could be estimated. The process is mentioned here only for completeness. However, the radiation should qualitatively resemble the impulsive emissions calculated for the imploding sphere in Section 5.2 on electrostatic sound. Similar objections could be raised about the impulsive nature of such a source.

8. SUMMARY AND CONCLUSIONS

8.1 Relative Merits of the Models

The simple-source models predict the radiation of a pressure pulse of about the same duration as the growth phase of a convection cell -- quite different in character from the observed infrasound. There is no experimental evidence that fluctuations on shorter time scales emit coherently over the spatial extent of a storm. However, fluctuations in the amplitude of infrasound measured both in the ionosphere and on the ground do exhibit a tendency toward a 20 to 30 min periodicity which has previously been attributed to storm life cycle (Georges, 1973).

Fluctuations on smaller spatial scales would emit sound, but their contributions would add incoherently over the extent of the storm. The strength and spectral content of such emissions are best modeled stochastically: A turbulent-emission model predicts an average radiated power spectral density proportional to $f^{-7/2}$, with most of the emitted power concentrated at frequencies corresponding to the outer scale of the turbulence. Realistic velocity fluctuations of 25 to 40 m s^{-1} extending over a 10 km-cube storm volume would radiate a total broadband power of 10^8 to 10^9 W. The spatial and temporal scales of these fluctuations (the turbulent outer scale) would cause the radiation to be strongest at 20 to 30 min wave periods and considerably weaker at the tens of seconds periods observed. Also, such a model cannot explain the observed trains of narrow-band infrasound sometimes observed.

The thermo-mechanical mechanisms appear not to be applicable to severe storms, because the heat-release mechanism (condensation) is always out of phase with wave-associated temperature fluctuations.

The electrical models appear to provide insufficient power in the observed spectral region; furthermore, it is difficult to explain the nearly continuous wave trains observed in terms of an essentially impulsive source. Enough uncertainty remains, however, that an experimental test would be desirable.

8.2 A "Most Likely" Model

The close association of infrasound with tornadic storms and the degree with which the theoretical model of vortex radiation matches the observations make the vortex-sound mechanism the "most likely" candidate. The observation that the infrasound seems to be related to tornado formation, but in some cases precedes it (Georges and Greene, 1975), along with the calculations of the vortex size required to match the observed radiated power and frequency, suggest that the rotating columns of air inside some thunderstorms called "tornado cyclones" may be the infrasound emitters. Radar observations show that tornado cyclones form up inside storms as much as an hour before tornadoes touch ground. (Note that Georges and Greene (1975) report that

infrasonic emissions often precede observed tornadoes by up to an hour.) Evidence from the deviation and curvature of tornado tracks (especially multiple tornadoes) suggest that the tornadoes may be satellite vortices of the moving longer tornado cyclone, as suggested by Agee et al. (1976). But whether or not tornadoes that reach the ground actually form from a given meso-cyclone, the infrasound radiating mechanism should operate.

However, the quasi-random character that some of the observed emissions assume suggests that some features of the turbulent source model are also relevant. The two models are not incompatible. A "hybrid" model, combining features of each, in fact appears to reproduce the most features of the observations. The actual radiation process could involve up to several individual vortex radiators at various stages of growth and decay inside a single storm complex (but not necessarily in a single storm cell). Many times, as is observed, a single source could dominate, radiating nearly monochromatically. At other times, the emissions may be the superposition of many sources. The key hypothesis that joins the two mechanisms is that the two are fundamentally the same physical process, but are only described differently. A very large number of randomly distributed eddies or vortices approaches what would normally be called turbulence, and their total radiation could only be computed statistically. Averaged over many storm events, then, the radiation would obey the spectral predictions of the turbulent model; for example, the average radiated power spectrum would follow an $f^{-7/2}$ law down to wave periods corresponding to storm-scale motions, i.e., 20 to 30 min. At the other extreme, a single vortex that degenerates in an orderly way can be modeled analytically and its radiation calculated exactly. The situation that we encounter in nature seems to lie between these two extremes, where neither model is completely satisfactory, but in different senses, each is. This aspect of the model needs to be refined by being placed on firm analytical ground.

Application of the simple model for the acoustic radiation from a corotating vortex pair to the problem of thunderstorm radiation provides a bridge between two different approaches to the problem. On one hand, there are completely deterministic models of coherent acoustic emissions based on certain storm processes known to resemble fluid monopole and dipole sources; on the other hand, it is possible to model the flow inside a storm stochastically, that is, as "turbulence" and to estimate the acoustic radiation according to Lighthill's model based on a random distribution of acoustic quadrupoles. The disadvantage of the former kind of model is that most of the phenomena inside storms that we know about and can model deterministically lead to the radiation of impulses only, or at least lead to very much longer period radiation than we require. The disadvantage of a stochastic approach is that it masks most of the physics that would relate storm processes to the emissions. The vortex-sound model provides what is needed: a basic radiating mechanism that can predict either coherent or incoherent emissions (both are observed), depending on the size and number of individual emitters inside a storm and their lifetimes.

8.3 Some Observational Tests

The electrical mechanisms lend themselves to tests that observe simultaneously the infrasonic and electromagnetic energy that storms radiate. For example, if the infrasound is part of the acoustic remnant of the cylindrical shock generated by lightning strokes, then there should be a spatial and temporal correlation between the infrasound sources and the sources of "atmospherics," the radio-frequency electromagnetic energy radiated by lightning. Such a test has been performed and is reported by Beasley et al. (1976), with negative results. Their results also show that other electromagnetic mechanisms (like the electrostatic-relaxation process) are also unlikely explanations for the observed infrasound.

The vortex-sound mechanism suggests several tests. Again, simultaneous mapping of an emitting storm's velocity field with high-resolution Doppler radar would permit a direct association between the radiation and the dynamics and structure of mesoscale vortices inside storms. The several Doppler and dual-Doppler meteorological radars now coming into operation increase the chances that such simultaneous observations will eventually happen (Figure 12).

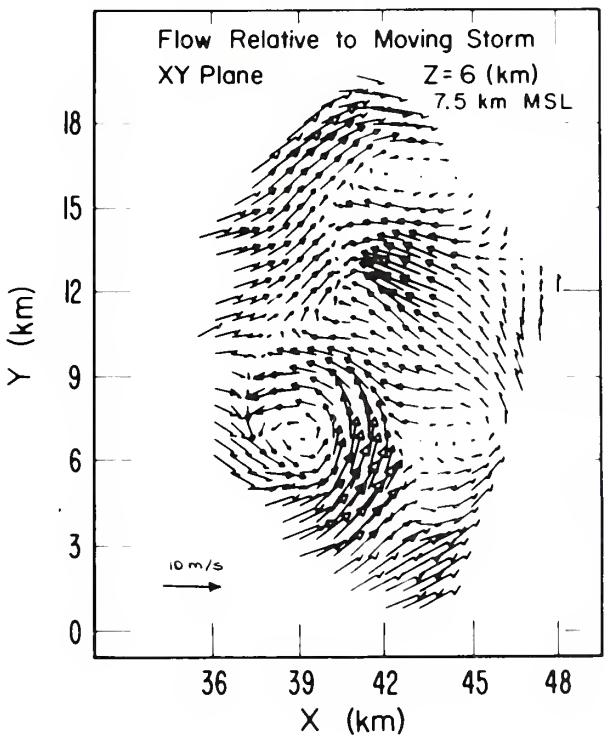

Figure 12. A map of horizontal air-velocity vectors at an altitude of 6 km above ground inside a Colorado thunderstorm. The velocity field was mapped with the WPL dual-Doppler radar (Kropfli and Miller, 1976). The length (and intensity) of each vector is proportional to air speed, with mean removed, at that location, with the highest speeds reaching 10 m s^{-1}. A strong vortex is visible at lower left, and two weaker ones at the top and at the lower right can also be seen. The radar resolution does not allow the sub-vortex structure to be seen with any detail.

If the infrasound is radiated from vertical vortices, the radiation should have directional characteristics that could be observed with sensors spaced azimuthally around the source. Azimuthal (rotational) symmetry in the source would be reflected in radiation that is nondirectional, except possibly for small time delays that may be detectable. Variability of propagation time would make this difficult, however. Azimuthal vortex asymmetries, such as those observed by Agee et al. (1975) could cause azimuthal variations in radiated frequency that may follow a predictable (and observable) pattern. Frequency-time spectra of emissions recorded at many observatories spaced in azimuth could reveal such patterns.

Another test has been devised to measure the radiation from a more accessible form of atmospheric vortex: dust devils. There is photographic evidence that dust devils exhibit multiple-vortex and turbulent structures (Figure 13). Calculations using the formulas of Section 6.3.1 show that dust-devil emissions should be detectable with existing infrasonic microphones. We attempted such an experiment but found no emissions that could be attributed unambiguously to several large dust devils that passed near our micro-

Figure 13. Photograph (by the author) of a dust-devil near Phoenix, Ariz., showing helical structure. Motion pictures of the same dust-devil reveal satellite vortices embedded in the flow.

phones. However, man-made interference, low equipment sensitivity and the small number of dust devils sampled could easily explain our negative result. More extensive experiments should be done.

If monopole or dipole oscillations of storm scale existed with sufficient intensity and at the right frequency to explain the infrasound observations, we would expect to observe corresponding large near-field (non-radiated) infrasonic pressure fluctuations in the vicinity of the emitting storms. It should be straightforward to estimate the expected near-field intensity and then either to examine existing pressure records (most of which, however, may not respond at the infrasonic frequencies) or to devise a simple sensor to detect them.

9. REFERENCES

Abdullah, A. J., The "musical" sound emitted by a tornado, *Mon. Weather Rev.*, 94, 213-220, 1966.

Abe, M., Cinematographic studies of rotary motions of a cloud mass near Mt. Fuji, *Geophys. Mag.* (Tokyo), 1, 211-223, 1923.

Agee, E., C. Church, C. Morris and J. Snow, Some synoptic aspects and dynamic features of vortices associated with the tornado outbreak of 3 April 1974, *Mon. Weather Rev.*, 103, 318-333, 1975.

Agee, E. M., J. T. Snow and P. R. Clarke, Multiple vortex features in the tornado cyclone and the occurrence of tornado families, *Mon. Weather Rev.*, 104, 552-563, 1976.

Anderson, C. E., A study of the pulsating growth of cumulus clouds, Geophysical Research Paper No. 72, AFCRL, Bedford, Mass., 1960.

Atlas, D. and Collaborators, Severe local storms, *Meteorological Monographs*, 5, 247 pp., American Meteorological Society, Boston, 1963.

Beasley, W. H., T. M. Georges and M. W. Evans, Infrasound from convective storms. Part V. An experimental test of electrical source mechanisms, *J. Geophys. Res.*, 81, 3133-3140, 1976.

Bhartendu, Sound pressure of thunder, *J. Geophys. Res.*, 76, 3515-3516, 1971.

Bowman, H. A. and A. J. Bedard, Observations of infrasound and subsonic pressure disturbances related to severe weather, *Geophys. J. Roy. Astron. Soc.*, 1971.

Brown, R. A., W. C. Bumgarner, K. C. Crawford and D. Sirmans, Preliminary Doppler velocity measurements in a developing radar hook-echo, *Bull. Amer. Meteorol. Soc.*, 52, 1186-1188, 1971.

Brown, R. A., D. W. Burgess and K. C. Crawford, Twin tornado cyclones within a severe thunderstorm: Single Doppler radar observations, *Weatherwise*, 26, 63-69, 1973.

Brown, R. A. and K. C. Crawford, Doppler radar evidence of severe storm high-reflectivity cores acting as obstacles to airflow, Proc. Fifteenth AMS Radar Meteorology Conf. 16-21, 1972.

Browning, K. A., Airflow and precipitation trajectories within severe local storms which travel to the right of the winds, *J. Atmos. Sci.*, 21, 634-639, 1964.

Browning, K. A., J. C. Fankhauser, J.-P. Chalon, P. J. Eccles, R. G. Strauch, F. H. Merrem, D. S. Musil, E. L. May and W. R. Sand, Structure of an evolving hailstorm, Part V: Synthesis and implications for hail growth and hail suppression, *Mon. Weather Rev.*, 104, 603-610, 1976.

Byers, H. R. and R. R. Braham, Jr., *The Thunderstorm*, U.S. Govt. Printing Off., Washington, D.C., 1949, NTIS Order No. PB 234 515.

Chalmers, J. A., *Atmospheric Electricity* (2nd Ed.), Pergamon Press, N.Y., 1967.

Chalon, J.-P., J. C. Fankhauser and P. J. Eccles, Structure of an evolving hailstorm, Part I: General characteristics and cellular structure, *Mon. Weather Rev.*, 104, 564-575, 1976.

Chanaud, R. C., Experimental study of aerodynamic sound from a rotating disc, *J. Acoust. Soc. Amer.*, 45, 392-397, 1969.

Chandrasekhar, S., *Hydrodynamic and Hydromagnetic Stability*, Oxford Press, London, 1961.

Chopra, K. P., Atmospheric and oceanic flow problems introduced by islands, *Advances in Geophysics*, 16, 297-421, 1973.

Chopra, K. P. and L. F. Hubert, Kármán vortex-streets in the earth's atmosphere, *Nature*, 203, 1341-1343, 1964a.

Chopra, K. P. and L. F. Hubert, Mesoscale eddies in the wake of islands, *J. Atmos. Sci.*, 22, 652-657, 1964b.

Cole, J. E. and R. A. Dobbins, Propagation of sound through atmospheric fog, *J. Atmos. Sci.*, 27, 426-434, 1970.

Colgate, S. A. and C. McKee, Electrostatic sound in clouds and lightning, *J. Geophys. Res.*, 74, 5379-5389, 1969.

Daniels, F. B., Lenghtening of shock waveforms caused by their propagation to high altitudes, *J. Acoust. Soc. Amer.*, 45, 241-242, 1969.

Darkow, G. L., Periodic tornado production by long-lived thunderstorms, Proc. Seventh AMS Conf. Severe Local Storms, 214-217, 1971.

Davies-Jones, R. P., The dependence of the core radius on swirl ratio in a tornado simulator, *J. Atmos. Sci.*, 30, 1427-1430, 1973.

Davies-Jones, R. P. and E. Kessler, Tornadoes, Ch. 16 in *Weather and Climate Modification*, (W. N. Hess, Ed.), Wiley, N.Y., 1974.

Davy, A., R. C. DiPrima and J. T. Stuart, On the instability of Taylor vortices, *J. Fluid Mech.*, 31, 17-52, 1968.

Dessler, A. J., Infrasonic thunder, *J. Geophys. Res.*, 78, 1889-1896, 1973.

Donaldson, R. J., Vortex signature recognition by a Doppler radar, *J. Appl. Meteor.*, 9, 661-670, 1970.

Eagleman, J. R. and V. U. Muirhead, Observed damage from tornadoes and safest location in houses, Proc. Seventh AMS Conf. Severe Local Storms, 171-178, 1971.

Einaudi, F. and D. P. Lalas, The propagation of acoustic-gravity waves in a moist atmosphere, *J. Atmos. Sci.*, 30, 365-376, 1973.

Fawbush, E. J., R. C. Miller, and L. G. Starrett, An empirical method of forecasting tornado development, *Bull. Amer. Meteorol. Soc.*, 32, 1-9, 1951.

Few, A. A., A. J. Dessler, D. J. Latham and M. Brook, A dominant 200-Hertz peak in the acoustic spectrum of thunder, *J. Geophys. Res.*, 72, 6149-6154, 1967.

Few, A. A., Power spectrum of thunder, *J. Geophys. Res.*, 74, 6926-6934, 1969.

Fujita, T., The Lubbock tornadoes: A study of suction spots, *Weatherwise*, 23, 160-173, 1970.

Fujita, T. T., Proposed mechanism of suction spots accompanied by tornadoes, Proc. Seventh AMS Conf. Severe Local Storms, 208-213, 1971.

Fujita, T. T., Proposed mechanism of tornado formation from rotating thunderstorm, Proc. Eighth AMS Conf. Severe Local Storms, 191-196, 1973.

Fujita, T. and J. Arnold, Development of a cumulonimbus under the influence of strong vertical shear, Proc. 10th AMS Weather Radar Conf. 178-186, 1963.

Fujita, T. and H. Grandoso, Split of a thunderstorm into anticyclonic and cyclonic storms and their motion as determined from numerical model experiments, *J. Atmos. Sci.*, 25, 416-439, 1968.

Fulks, J. R., On the mechanics of the tornado, Natl. Severe Storms Proj. Rept. No. 4, U.S. Weather Bureau, 1962.

Georges, T. M., Infrasound from convective storms: examining the evidence, *Reviews of Geophysics and Space Physics*, 11, 571-594, 1973.

Georges, T. M. and G. E. Greene, Infrasound from convective storms: Pt. IV. Is it useful for storm warning? *J. Appl. Meteorol.*, 14, 1303-1316, 1975.

Georges, T. M., and W. H. Beasley, Refraction of infrasound by upper-atmospheric winds, (in preparation), 1976.

Goldman, J. L. and E. M. Wilkins, Drag experiments with cylinders of varying roughness related to flow around thunderstorm cells, *J. Geophys. Res.*, 78, 913-919, 1973.

Holmes, C. R., M. Brook, P. Krehbiel and R. McCrory, On the power spectrum and mechanism of thunder, *J. Geophys. Res.*, 76, 2106-2115, 1971a.

Holmes, C. R., M. Brook, P. Krehbiel and R. McCrory, Reply, *J. Geophys. Res.*, 76, 7443, 1971b.

Idso, S., Whirlwinds, density currents and topographic disturbances: a meteorological melange of intriguing interactions, *Weatherwise*, 28, 61-65, 1975.

Jessup, E. A., Interpretations of chaff trajectories near a severe thunderstorm, *Mon. Weather Rev.*, 100, 653-661, 1972.

Jones, D. L., G. G. Goyer and M. N. Plooster, Shock wave from a lightning discharge, *J. Geophys. Res.*, 73, 3121-3127, 1968.

Kelvin, Lord, Vibrations of a columnar vortex, in *Mathematical and Physical Papers*, Cambridge Univ. Press, 152-165, 1910, or *Phil. Mag.*, 5, 155-168 (1880).

Kraus, M. J., Doppler radar observations of the Brookline, Massachusetts, tornado of 9 August 1972, *Bull. Amer. Meteorol. Soc.*, 54, 519-524, 1973.

Kropfli, R. A. and L. J. Miller, Kinematic structure and flux quantities in a convective storm from dual-Doppler radar observations, *J. Atmos. Sci.*, 33, 520-529, 1976.

Kropfli, R. A. and L. J. Miller, Thunderstorm flow patterns in three dimensions, *Mon. Weather Rev.*, 103, 70-71, 1975.

Lamb, H., *Hydrodynamics*, Dover, New York, 1945.

Lemon, L. R., Wake vortex structure and aerodynamic origin in severe thunderstorms, *J. Atmos. Sci.*, 33, 678-685, 1976.

Lemon, L. R., D. W. Burgess and R. A. Brown, Tornado production and storm sustenance, Proc. Ninth AMS Conf. Severe Local Storms, 100-104, 1974.

Letzman, J., Cumulus pulsations, *Meteorol. Zeits.*, 47, 236-238, 1930.

Lighthill, M. J., On sound generated aerodynamically, Part 1, General theory, *Proc. Roy. Soc. London A*, 211, 564-587, 1952.

Lighthill, M. J., On sound generated aerodynamically, Part 2, Turbulence as a source of sound, *Proc. Roy. Soc. London A*, 222, 1-32, 1954.

Lighthill, M. J., Sound generated aerodynamically, *Proc. Roy. Soc. London A*, 267, 147-182, 1962.

Ludlam, F. H., Severe local storms: a review, in Severe Local Storms, *Meteorol. Monogr.*, 5, 1-30, American Meteorological Society, 1963.

Lumley, J. L. and H. A. Panofsky, *The Structure of Atmospheric Turbulence*, John Wiley, New York, 1964.

Marble, F. E., Some gas dynamic problems in the flow of condensing vapors, *Astronaut. Acta*, 14, 585-614, 1969.

Marble, F. E. and D. C. Wooten, Sound attenuation in a condensing vapor, *Phys. Fluids*, 13, 2657-2664, 1970.

Mawardi, O. K., Aero-thermoacoustics (the generation of sound by turbulence and by heat processes), *Rpt. Prog. Phys.*, 19, 156-186, 1956.

Meecham, W. C. and G. W. Ford, Acoustic radiation from isotropic turbulence, *J. Acoust. Soc. Amer.*, 30, 318-322, 1958.

Merk, H. J., Analysis of heat-driven oscillations of gas flows. I. General considerations, *Appl. Sci. Res.*, 6, 317-336, 1956.

Morse, P. and K. Ingard, *Theoretical Acoustics*, McGraw-Hill, New York, 1968.

Morton, B. R., Geophysical vortices, Ch. 6 in *Progress in Aeronautical Sciences*, 7, 145-193, 1966.

Newton, C. W., Dynamics of severe convective storms, in Severe Local Storms, *Meteorol. Monogr.*, 5, 33-58, American Meteorological Society, Boston 1963.

Newton, C. W., Circulations in large sheared cumulonimbus, *Tellus*, 18, 699-713, 1966.

Newton, C. W., Severe convective storms, *Advances in Geophysics*, 12, 257-308, 1967.

Newton, C. W. and H. R. Newton, Dynamical interactions between large convective clouds and environment with vertical shear, *J. Meteorol.*, 16, 483-496, 1959.

Pierce, A. D. and S. C. Coroniti, A mechanism for the generation of acoustic-gravity waves during thunderstorm formation, *Nature*, 210, 1209-1210, 1966.

Phillips, O. M., The intensity of aeolian tones, *J. Fluid Mech.*, 1, 607-624, 1956.

Powell, A., On the edgetone, *J. Acoust. Soc. Amer.*, 33, 395-409, 1961.

Powell, A., Theory of vortex sound, *J. Acoust. Soc. Amer.*, 36, 177-195, 1964.

Prasad, S. S., L. J. Schneck and K. Davies, Ionospheric disturbances by severe tropospheric weather storms, *J. Atmos. Terrest. Phys.*, 37, 1357-1363, 1975.

Priestley, C. H. B., Buoyant motion in a turbulent environment, *Austral. J. Phys.*, 6, 279-290, 1953.

Procunier, R. W. and G. W. Sharp, Optimum frequency for detection of acoustic sources in the upper atmosphere, *J. Acoust. Soc. Amer.*, 49, 622-626, 1971.

Proudman, I., The generation of noise by isotropic turbulence, *Proc. Roy. Soc. London*, A214, 119-132, 1952.

Putnam, A. A. and W. R. Dennis, Survey of organ-pipe oscillations in combustion systems, *J. Acoust. Soc. Amer.*, 28, 246-259, 1956.

Rayleigh, Lord, Explanation of certain acoustical phenomena, Roy. Inst. Proc. VIII, 536-542, 1878; Nature XVIII, 319-321, 1878; Reprinted in *Scientific Papers of Lord Rayleigh*, Dover, N.Y., 1964.

Rayleigh, Lord, Acoustical observations. II, *Phil. Mag.* VII, 149-162, 1879; Reprinted in *Scientific Papers of Lord Rayleigh*, Dover, N.Y., 1964.

Reed, J. W., Attenuation of blast waves by the atmosphere, *J. Geophys. Res.*, 77 1616-1622, 1972.

Reed, S. G., Jr., Note on finite amplitude propagation effects on shock wave travel times from explosions at high altitude, *J. Acoust. Soc. Amer.*, 31, 1265, 1959.

Remillard, W. J., The acoustics of thunder, Tech. Memo. No. 44, Acoustics Res. Lab. Harvard Univ., Cambridge, Mass., 1960.

Richardson, E. G., Aeolian tones, *Proc. Phys. Soc. London*, 36, 153-167, 1924.

Rijke, P. R., On the vibration of the air in a tube open at both ends, *Pogg. Ann.* CVII, 339, 1859.

Scorer, R. S. and F. H. Ludlam, Bubble theory of penetrative convection, *Q. J. Roy. Meteorol. Soc.*, 79, 94-103, 1953.

Stein, R. F., Generation of acoustic-gravity waves by turbulence in an isothermal stratified atmosphere, *Solar Physics*, 2, 385-432, 1967.

Strauch, R. G., A. S. Frisch and W. B. Sweezy, Doppler radar measurements of turbulence, shear and dissipation rates in a convective storm, Proc. 16th AMS Radar Meteorol. Conf. 83-88, 1975.

Turner, J. S., Jets and plumes with negative or reversing buoyancy, *J. Fluid Mech.*, 26, 779-792, 1966.

Uman, M. A., *Lightning*, McGraw-Hill, New York, 1969.

Ward, N. B., The exploration of certain features of tornado dynamics using a laboratory model, *J. Atmos. Sci.*, 29, 1194-1204, 1972.

Weske, J. R. and T. M. Rankin, Generation of secondary motions in the field of a vortex, *Phys. Fluids*, 6, 1397-1403, 1963.

Wilkins, E. M., Hot-film anemometer measurements of velocity decay in Karman trail vortexes, *J. Geophys. Res.*, 75, 1033-1039, 1970.

Workman, E. J. and S. E. Reynolds, Time of rise and fall of cumulus cloud tops, *Bull. Amer. Meteorol. Soc.*, 30, 359-361, 1949.

Yih, C.-S., *Fluid Mechanics*, McGraw-Hill, N.Y., 1969.

Zimmerman, L. I., Atmospheric wake phenomena near the Canary Islands, *J. Appl. Meteorol.*, 8, 896-907, 1969.

☆ U.S. Government Printing Office: 1976-777-045/ 1203 Region

Environmental Research LABORATORIES

The mission of the Environmental Research Laboratories (ERL) is to conduct an integrated program of fundamental research, related technology development, and services to improve understanding and prediction of the geophysical environment comprising the oceans and inland waters, the lower and upper atmosphere, the space environment, and the Earth. The following participate in the ERL missions:

MESA *Marine EcoSystems Analysis Program.* Plans, directs, and coordinates the regional projects of NOAA and other federal agencies to assess the effect of ocean dumping, municipal and industrial waste discharge, deep ocean mining, and similar activities on marine ecosystems.

OCSEA *Outer Continental Shelf Environmental Assessment Program.* Plans, directs, and coordinates research of federal, state, and private institutions to assess the primary environmental impact of developing petroleum and other energy resources along the outer continental shelf of the United States.

WM *Weather Modification Program Office.* Plans, directs, and coordinates research within ERL relating to precipitation enhancement and mitigation of severe storms. Its National Hurricane and Experimental Meteorology Laboratory (NHEML) studies hurricane and tropical cumulus systems to experiment with methods for their beneficial modification and to develop techniques for better forecasting of tropical weather. The Research Facilities Center (RFC) maintains and operates aircraft and aircraft instrumentation for research programs of ERL and other government agencies.

AOML *Atlantic Oceanographic and Meteorological Laboratories.* Studies the physical, chemical, and geological characteristics and processes of the ocean waters, the sea floor, and the atmosphere above the ocean.

PMEL *Pacific Marine Environmental Laboratory.* Monitors and predicts the physical and biological effects of man's activities on Pacific Coast estuarine, coastal, deep-ocean, and near-shore marine environments.

GLERL *Great Lakes Environmental Research Laboratory.* Studies hydrology, waves, currents, lake levels, biological and chemical processes, and lake-air interaction in the Great Lakes and their watersheds; forecasts lake ice conditions.

GFDL *Geophysical Fluid Dynamics Laboratory.* Studies the dynamics of geophysical fluid systems (the atmosphere, the hydrosphere, and the cryosphere) through theoretical analysis and numerical simulation using powerful, high-speed digital computers.

APCL *Atmospheric Physics and Chemistry Laboratory.* Studies cloud and precipitation physics, chemical and particulate composition of the atmosphere, atmospheric electricity, and atmospheric heat transfer, with focus on developing methods of beneficial weather modification.

NSSL *National Severe Storms Laboratory.* Studies severe-storm circulation and dynamics, and develops techniques to detect and predict tornadoes, thunderstorms, and squall lines.

WPL *Wave Propagation Laboratory.* Studies the propagation of sound waves and electromagnetic waves at millimeter, infrared, and optical frequencies to develop new methods for remote measuring of the geophysical environment.

ARL *Air Resources Laboratories.* Studies the diffusion, transport, and dissipation of atmospheric pollutants; develops methods of predicting and controlling atmospheric pollution; monitors the global physical environment to detect climatic change.

AL *Aeronomy Laboratory.* Studies the physical and chemical processes of the stratosphere, ionosphere, and exosphere of the Earth and other planets, and their effect on high-altitude meteorological phenomena.

SEL *Space Environment Laboratory.* Studies solar-terrestrial physics (interplanetary, magnetospheric, and ionospheric); develops techniques for forecasting solar disturbances; provides real-time monitoring and forecasting of the space environment.

U.S. DEPARTMENT OF COMMERCE
National Oceanic and Atmospheric Administration
BOULDER, COLORADO 80302